

# SINGLE PARTICLE DEGREES OF FREEDOM IN THE INTERACTING BOSON MODEL

O. SCHOLTEN

*Cyclotron Laboratory and Department of Physics Astronomy, Michigan State University, East Lansing, MI 48824, U.S.A.*

**Abstract**—An overview is given of different aspects of the Interacting Boson Fermion Model, the extension of the interacting Boson Model to odd mass nuclei. The microscopic model for the coupling of single-particle degrees of freedom to the system of bosons is outlined and the interaction between the bosons and the single-particle is derived. The predictions of the model are compared to those of the standard geometrical models. As realistic examples calculations of the low-lying positive and negative parity states in the odd-mass Europium isotopes and of the spreading width of deeply-bound hole states in the odd-mass Palladium isotopes are presented. The concept of dynamical super-symmetries is outlined. Also the phenomenology and microscopy of the coupling of two-quasi-particles to the bosons is discussed.

## CONTENTS

1. INTRODUCTION	190
2. MICROSCOPIC FORMULATION: EVEN-EVEN NUCLEI	191
2.1. Generalized seniority	191
2.2. The OAI method	193
2.3. Deformed nuclei	194
2.4. The IBA Hamiltonian	194
3. MICROSCOPIC FORMULATION: ODD-MASS NUCLEI	196
3.1. Definition of the model basis space	196
3.2. Construction of the Quadrupole operator	196
3.2.1. <i>Direct mapping</i>	197
3.2.2. <i>Nuclear field theory</i>	198
3.2.3. <i>Quasi-particles</i>	199
3.3. The IBFA Hamiltonian	201
3.4. Relation to other quasi-particle-core coupling models	202
4. PHENOMENOLOGY	203
4.1. Geometrical limits	203
4.1.1. <i>The SU (5) limit</i>	204
4.1.2. <i>The SU (3) limit</i>	205
4.1.3. <i>The O (6) limit</i>	209
4.2. The Europium isotopes	211
4.3. Spreading width of deeply bound hole states	217
5. BOSON-FERMION SYMMETRIES	218
6. TWO QUASI-PARTICLE DEGREES OF FREEDOM	221
6.1. Microscopic treatment	221
6.2. Some applications	223
6.2.1. <i>Low spin states</i>	223
6.2.2. <i>High spin states</i>	224
6.3. Giant resonances	225
7. SUMMARY	226
ACKNOWLEDGEMENTS	227
REFERENCES	227

## 1. INTRODUCTION

In the Interacting Boson Approximation (IBA) model the properties of low-lying collective states are calculated in terms of a system of interacting  $s$  and  $d$  bosons. In this form it was first formulated by Iachello and Arima.<sup>(1)</sup> It differs from most other boson models by the explicit introduction of an  $s$  ( $J^\pi = 0^+$ ) boson in addition to the usual quadrupole phonon ( $J^\pi = 2^+$ ) in such a way that the total number of  $s$ - and  $d$ -bosons is a conserved and finite number. It can be shown that the  $s$ -boson (or equivalently the factors  $\sqrt{N-n_d}$  in Ref. 5) account for much of the effect of the Pauli principle acting on the finite number of valence nucleons. Another consequence is that the model has a definite group structure which allows for the introduction of the concept of dynamical symmetries<sup>(2,3,4)</sup> furthermore since the model space is finite dimensional exact calculations are possible. This model has proved to be very successful in many phenomenological applications<sup>(6)</sup> to nuclei ranging from spherical<sup>(2)</sup> to deformed<sup>(3)</sup> to gamma-unstable,<sup>(4)</sup> to nuclei varying in mass from as light as <sup>(7)</sup>  $A = 18$  to as heavy as <sup>(8)</sup>  $A = 238$ , and for several transitional nuclei in between these limits.<sup>(9-11)</sup>

Shortly after the introduction of the phenomenological IBA model (until then called the Interacting Boson Model, IBM) a microscopic foundation was introduced,<sup>(12,13)</sup> in which the boson was interpreted as a collective fermion pair state. The  $s$ -boson is seen as the equivalent of a collective  $J^\pi = 0^+$  fermion ( $S^-$ ) pair state while the  $d$ -boson is seen as the equivalent of a collective fermion pair state with angular momentum  $J^\pi = 2^+$  ( $D$ -pair). This picture directly links the IBA model to the Generalized Seniority (GS) scheme,<sup>(14)</sup> which has contributed much to the qualitative understanding of the dependence of the model parameters on particle number.<sup>(15,16)</sup> One immediate<sup>(12)</sup> consequence of this relation between fermion pair states and the bosons is that the number of bosons should be taken equal to the number of fermion pairs in the valence shells.

By coupling single particle (s.p.) degrees of freedom to the system of bosons the IBA model can be extended to the Interacting Boson Fermion Approximation<sup>(17,18)</sup> (IBFA) model in which odd- $A$  nuclei can be described. This extension has two important consequences; (i) it allows for a relatively simple phenomenological description of the complicated spectra of odd-mass nuclei and (ii) the coupling of the single particle degrees of freedom depends sensitively on the detailed structure of the bosons<sup>(42)</sup> which makes the odd-mass nuclei the ultimate test-ground for microscopic theories of the IBA model. In this paper some examples of the successes and shortcomings of the IBFA model will be mentioned.

The model can be extended one step further by coupling two quasi-particle degrees of freedom to the bosons. In this way high spin phenomena such as backbending<sup>(90-92)</sup> and even giant resonances can be described.<sup>(87-89)</sup> Also in the low-lying part of the spectrum non  $s$ - $d$  boson degrees of freedom can play an important role. Clear cases are the negative parity states which are built on a collective  $J^\pi = 3^-$  state and can be calculated in the IBA model by coupling a  $f$ -boson to the system of  $s$ - and  $d$ -bosons.<sup>(9)</sup> Other examples are low-lying (around 1.5 MeV)  $K^\pi = 3^+$  bands in deformed nuclei which can be accounted for by coupling a  $J^\pi = 4^+$  (g) pair state<sup>(83-86)</sup> to the IBA bosons.

The relation between the IBA model and the Generalized Seniority scheme is discussed in Section 2 and the microscopic basis is laid for the coupling of the particle degrees of freedom to the bosons. The first problem one encounters in coupling the particle degrees of freedom to the bosons is a proper definition of the model space which is discussed in the first part of Section 3. The dominant part of the interaction between the bosons originates from the

neutron–proton quadrupole–quadrupole interaction. For this reason in that section some approaches are outlined for constructing the image of the shell-model quadrupole operator in IBFA. It will be shown that in the IBFA model the quadrupole operator consists of three different terms, one that acts only on the odd particle, another one that acts only on the bosons and a mixed term. The first two terms contribute to a direct boson–fermion quadrupole interaction in the IBFA Hamiltonian while the last term gives rise to the exchange force. This force accounts for the fact that the bosons themselves are built up of fermions which can occupy some of the same single particle orbits which are coupled explicitly. In Section 4 some examples are worked out in which an odd-particle is coupled to a spherical, an axially symmetric and a gamma-unstable core. In these limiting cases the features of the weak-coupling and the Nilsson model are reproduced. As an illustration the model is applied to the odd-mass  ${}_{63}\text{Eu}$  isotopes. In another example the model is used to calculate the spreading width of deeply-bound neutron hole states in the  ${}_{46}\text{Pd}$  isotopes. The concept of dynamical symmetries for odd-mass nuclei is outlined in Section 5. A microscopic treatment of two quasi-particle states in the IBA model together with some examples is discussed in Section 6.

## 2. MICROSCOPIC FORMULATION: EVEN–EVEN NUCLEI

### 2.1. Generalized seniority

The fact that the bosons in the IBA model can be regarded as collective fermion pair states<sup>(12,15)</sup> introduces a natural link between the IBA model and the shell model. This link can be established most directly through the introduction of the Generalized Seniority (GS) scheme. A recent review of this relationship can be found in Ref. 19. For this reason only the most important aspects will be briefly mentioned here.

In the GS scheme<sup>(14)</sup> which can be regarded as a generalization of the conventional seniority scheme<sup>(20,21)</sup> to the case of several non-degenerate orbits, one introduces a pair creation operator,

$$S^\dagger = \sum \alpha_j S_j^\dagger, \quad S_j^\dagger = \frac{1}{2} \sqrt{2j+1} (c_j^\dagger c_j^\dagger)^{(0)}. \quad (2.1)$$

This operator creates a collective  $J = 0$  pair which can be regarded as a nuclear Cooper-pair.<sup>(15)</sup> In the conventional seniority scheme the operator  $S^\dagger$ , its hermitian conjugate  $S^-$  and their commutator  $S_0$  are the generators of a  $SU(2)$  lie algebra. This makes the seniority scheme easy to apply, since reduction formulas for matrix elements are readily constructed. This is no longer true for the generalized seniority scheme and an  $SU(2)$  algebra can only be constructed in this way for the special case in which  $\alpha_j = 1$ . The only possibility for constructing an  $SU(2)$  algebra for the general case is by introducing<sup>(22,23)</sup> the operator  $S^- = \sum \alpha_j^{-1} S_j^-$  and its commutator with  $S^\dagger$ . The operator  $S^-$  is however no longer the hermitian conjugate of  $S^\dagger$  which is less appealing for practical applications.

A state with generalized seniority  $w = 0$  and  $n = 2N$  particles can be expressed as

$$|n, J = 0, w = 0\rangle = (S^\dagger)^N |0\rangle. \quad (2.2)$$

For spherical and semi-closed shell nuclei the groundstate can be described to a good approximation by (2.2) with suitably<sup>(21,24)</sup> adjusted values for the coefficients  $\alpha_j$ . To describe an excited  $2^+$  state one introduces the operator

$$D^\dagger = \sum_{jj'} \frac{1}{2} \beta_{jj'} \sqrt{1 + \delta_{jj'}} (c_j^\dagger c_{j'}^\dagger)^{(2)} \quad (2.3)$$

which creates a collective state with  $J = 2, w = 2$ . A GS state with  $n = 2N$  particles and  $J = 2$  can then be constructed by operating with (2.3) on a state with  $n = 2N, w = 0$ ,

$$|n, J = 2, w = 2\rangle = D^\dagger(S^\dagger)^{N-1} |0\rangle. \quad (2.4)$$

The structure coefficients  $\alpha_j$  [eqn. (2.1)] and  $\beta_{ij}$  [eqn. (2.3)] of the collective pairs can be obtained by diagonalizing the shell model interaction in the space of all  $w = 2$  states.<sup>(21)</sup> Since this space is small (a typical dimension is 10) it does not require much calculational effort. Using similar expressions for  $J > 2$  the method can be generalized and used to calculate the spectrum of semi-magic nuclei.<sup>(24)</sup> In Fig. 1 the spectrum for  $^{144}_{62}\text{Sm}_{82}$

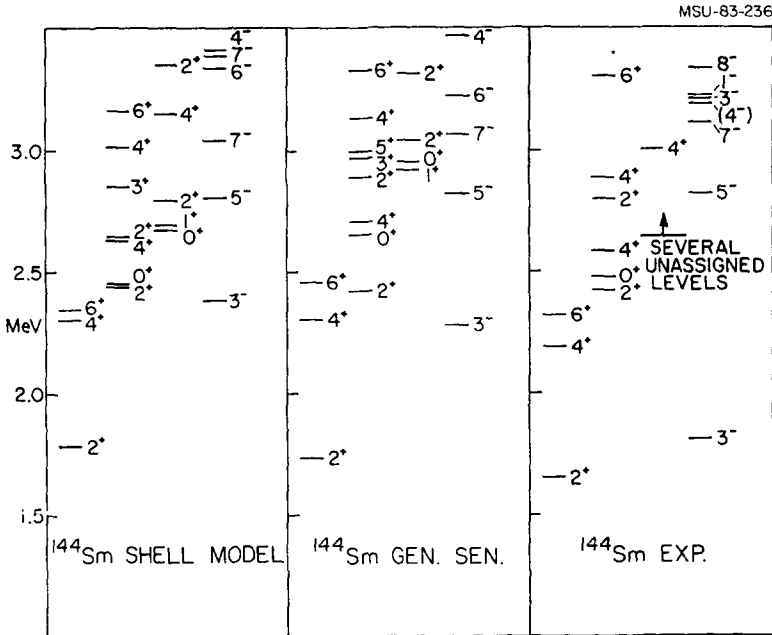


Fig. 1. The spectrum of  $^{144}\text{Sm}$  calculated in the Generalized seniority scheme is compared with a shell model calculation<sup>(25)</sup> and the experimental spectrum.<sup>(26)</sup>

calculated in the GS scheme is compared with a shell-model calculation<sup>(25)</sup> and experiment.<sup>(26)</sup> The interaction used in the GS calculation is the same as in the shell-model where it has been adjusted to reproduce the spectra of the  $N = 82$  isotones.<sup>(25)</sup> A typical dimension in this shell-model calculation is 2000. This comparison between the two calculations indicates that the GS scheme yields a powerful truncation scheme.

Because of the lack of an underlying symmetry group structure the quantum number  $w$  should be treated with some care. The state  $D^2S^{N-2} |0\rangle$  for  $J = 0$ , for example, has to be orthogonalized for each  $N$  explicitly to the state  $S^N |0\rangle$ , to obtain a state with  $w = 4$ . (In the conventional seniority scheme the results of this orthonormalization have a trivial  $N$ -dependence because of the underlying  $SU(2)$  group structure.) In actual calculations this  $N$ -dependent orthonormalization does not cause any severe drawbacks since mostly the interest is in the lowest seniority states. Some reduction formulas for the matrix elements of operators between low GS states are given in Ref. 27.

## 2.2. The OAI method

In 1978 Otsuka, Arima and Iachello<sup>(15)</sup> (OAI) introduced a method for relating the operators in the IBA model to those of the shell model. It differs from other methods in that it is not based upon a formal mapping between boson operators and shell model operators but rather emphasizes the equivalence between states in the two models. The states in the two spaces can be related most transparently if one works in the GS scheme. An IBA state with  $N$ -boson and with  $n_d$   $d$ -bosons corresponds to a shell model state with  $n = 2N$  and  $w = 2n_d$ . The shell model state (2.2) corresponds thus to the state  $(s^\dagger)^N |0\rangle$  in the IBA model, where  $s^\dagger$  is an  $s$ -boson creation operator. In this respect the  $S$ -pair operator is the shell model counterpart of the  $s$ -boson. The state (2.4) is the IBA model equivalent of the one  $d$ -boson state  $d^\dagger (s^\dagger)^{N-1} |0\rangle$ . The  $D$ -pair creation operator can thus be regarded as the microscopic counterpart of the  $d$ -boson.

Because of this particular relation between the shell model and the IBA model, operators are mapped from one space onto the other by requiring that the matrix elements of the operators are equal between equivalent states in the two model spaces.<sup>(15,16)</sup> As an example of this procedure we consider the matrix elements of the quadrupole operator. For simplicity we will work in the conventional seniority scheme instead of the GS scheme, since for the present purpose it is not essential. The shell model quadrupole operator can be written as

$$q^{(2)} = \sum Q_{jj'} (c_j^\dagger \tilde{c}_{j'})^{(2)} \quad (2.5)$$

where  $Q_{jj'}$  are the single particle matrix elements of the quadrupole operator  $Q_{jj'} = \langle j || r^2 Y_2(\hat{r}) || j' \rangle$ . The matrix elements of this operator can be calculated using seniority reduction formulas<sup>(28)</sup> as

$$\langle j^{2N}, v = 0, J = 0 || q^{(2)} || j^{2N}, v = 2, J = 2 \rangle = \sqrt{N(\Omega - N)/(\Omega - 1)} \langle j^2, v = 0, J = 0 || q^{(2)} || j^2, v = 2, J = 2 \rangle, \quad (2.6)$$

where  $\Omega$  is the pair degeneracy,  $\Omega = (2j + 1)/2$ . In the IBA model the quadrupole operator can to lowest order in the  $d$  boson operators be written as

$$Q_B = \kappa [(s^\dagger \tilde{d} + d^\dagger \tilde{s})^{(2)} + \chi (d^\dagger \tilde{d})^{(2)}]. \quad (2.7)$$

The matrix element corresponding to (2.6) in the IBA model is thus

$$\langle s^N || Q_B || s^{N-1} d \rangle = \sqrt{5N} \kappa. \quad (2.8)$$

Equating the matrix elements the left hand sides of eqns. (2.6) and (2.8) yields

$$\kappa = \sqrt{(\Omega - N)/(\Omega - 1)} \langle j^2, J = 0 || q^{(2)} || j^2, J = 2 \rangle / \sqrt{5}. \quad (2.9)$$

Following a similar procedure an expression for  $\chi$  can be derived. For large values of  $\Omega$  it can be shown<sup>(28)</sup> that the matrix element (2.6) depends on  $v$  as  $\sqrt{2N - v}$  while (2.8) depends on  $n_d$  as  $\sqrt{N - n_d}$ . Since  $v = 2n_d$  this shows the important role played by the  $s$ -boson in IBA.

The effect of the finite number of bosons can be studied in schematic models. One such exactly solvable schematic model is the  $O(4)$  model developed by Piepenbring *et al.*<sup>(101)</sup> This model simulates the pairing plus quadrupole force model. It is a single- $j$  model in which fermion seniority can be treated exactly. Matsuyanagi<sup>(102)</sup> has used this model to study the effects of a finite fermion space on matrix elements as a function of seniority and compared the results with the predictions following from the IBA model. His conclusion is that, if the number of particles is large ( $N \simeq \Omega$ ), the IBA model does not provide a satisfactory

reproduction of, for example, the transition matrix elements between levels with increasing seniority. The quenching of the transitions is less than is expected on the basis of a finite boson number. For smaller numbers, the cutoff effects agree much better with the results of the schematic  $O(4)$  model. It should be noted, however, that in the  $O(4)$  model angular momentum cannot be treated, which makes comparison with the IBA model less direct.

### 2.3. Deformed nuclei

The OAI procedure can be applied not only to spherical nuclei where the GS basis offers a valid truncation scheme, but also to deformed nuclei. In deformed nuclei a microscopic description of an intrinsic state can be provided by a deformed HFB calculation. Matrix elements of operators for this intrinsic state can be equated to those for coherent states in the IBA model.<sup>(29-31)</sup> Since the procedure for deformed nuclei has not yet been extended to the case of odd-mass nuclei this topic will not be discussed here.

### 2.4. The IBA Hamiltonian

In this section the IBA model will be discussed only briefly as it has been used in phenomenological applications to even-even nuclei.

The version closest to the microscopic picture is the IBA-2 model,<sup>(13,15)</sup> where one treats neutron and proton degrees of freedom explicitly. The Hamiltonian used with much success<sup>(6)</sup> in phenomenological applications to a wide range of nuclei can be written as

$$H_{II} = \varepsilon_{v\pi} \hat{n}_d + \kappa_{v\pi} Q_v^{(2)} \cdot Q_\pi^{(2)} + M_{v\pi} + V_{vv} + V_{\pi\pi} + E_0, \quad (2.10)$$

where

$$Q_\rho^{(2)} = (s_\rho^\dagger \tilde{d}_\rho + d_\rho^\dagger s_\rho)^{(2)} + \chi_\rho (d_\rho^\dagger \tilde{d}_\rho)^{(2)}; \quad \rho = v, \pi$$

$$M_{v\pi} = \xi_2 (s_v^\dagger d_\pi^\dagger - d_v^\dagger s_\pi^\dagger)^{(2)} \cdot (s_v \tilde{d}_\pi - \tilde{d}_v s_\pi)^{(2)} - 2 \sum_{k=1,3} \xi_k (d_v^\dagger d_\pi^\dagger)^{(k)} \cdot (\tilde{d}_v \tilde{d}_\pi)^{(k)}$$

and

$$V_{\rho\rho} = \sum_{L=0,2,4} \frac{1}{2} C_\rho^L (2L+1) [(d_\rho^\dagger d_\rho^\dagger)^{(L)} (\tilde{d}_\rho \tilde{d}_\rho)^{(L)}]^{(0)}$$

which is not the most general IBA-2 Hamiltonian. The first term gives the energy difference between the  $s$  and  $d$  boson. It arises from the fact that in the effective interaction between like particles the monopole pairing force is stronger than the quadrupole pairing force which gives more binding to the  $S$ -pair than the  $D$ -pair state. Although in principle the  $d$ -boson energies  $\varepsilon_{v\pi}$  can be different for neutron and proton bosons, they have for simplicity in phenomenological applications always been taken as equal. Since the major part of the interaction between like particles is already absorbed in the boson energies, the residual interaction between like bosons,  $V_{vv}$  and  $V_{\pi\pi}$ , is of minor importance. The  $Q_\pi^{(2)} \cdot Q_v^{(2)}$  interaction is the boson image of the (strong) neutron-proton quadrupole-quadrupole interaction. The Majorana force  $M_{v\pi}$  has the function to shift up the position of all states which are not totally symmetric in the neutron-proton degree of freedom. It can be shown<sup>(21)</sup> that this term in the effective boson interaction results from a truncation of the basis to  $s$ - and  $d$ -bosons only.

The simpler version of the model, IBA-1, was introduced first.<sup>(1)</sup> In this earlier version only one kind of  $s$ - and  $d$ -bosons are present and there is no distinction made between the

neutron and proton degrees of freedom in the nucleus. The Hamiltonian can be written in several different ways, the simplest of which for the present discussion is in terms of a multipole expansion,

$$H_I = \varepsilon \hat{n}_d + \kappa Q^{(2)} \cdot Q^{(2)} + \kappa' L^{(1)} \cdot L^{(1)} + \kappa'' O^{(3)} \cdot O^{(3)} + \kappa''' H^{(4)} \cdot H^{(4)} \quad (2.11)$$

where

$$\begin{aligned} Q^{(2)} &= (s^\dagger \tilde{d} + d^\dagger s)^{(2)} + \chi (d^\dagger \tilde{d})^{(2)} \\ L^{(1)} &= \sqrt{10} (d^\dagger \tilde{d})^{(1)} \\ O^{(3)} &= \sqrt{5} (d^\dagger \tilde{d})^{(3)} \\ H^{(4)} &= \sqrt{5} (d^\dagger \tilde{d})^{(4)}. \end{aligned}$$

In the multipole form of the Hamiltonian given in eqn. (2.11), the boson pairing force<sup>(9)</sup> has not been introduced but instead the parameter  $\chi$  has been used in the quadrupole operator. For  $\chi = -\frac{1}{2}\sqrt{7}$  the quadrupole operator is the same as is used in the multipole decomposition given in Ref. 9. If  $\chi = 0$  it resembles the pairing force of Ref. 9. The present formulation is based on the consistent  $Q$  formulation of Ref. 100. As is well known there are three possible dynamical symmetries in the IBA model. The  $U(5)$  symmetry<sup>(2)</sup> is realized by putting  $\kappa = 0$ , the  $U(3)$  symmetry<sup>(3)</sup> by putting  $\varepsilon = \kappa'' = \kappa''' = 0$  and  $\chi = \pm\frac{1}{2}\sqrt{7}$  and the  $O(6)$  symmetry<sup>(4)</sup> by  $\varepsilon = \kappa''' = \chi = 0$ .

Since no distinction is made between neutron and proton degrees of freedom the model space of the IBA-1 model is an order of magnitude smaller than that of the IBA-2 model. For this reason it is easier to use in numerical applications and is easier to extend to include other degrees of freedom such as the single particle degrees of freedom which are discussed in this article. In spite of its very limited model space it appears that the IBA-1 model describes the low-lying collective states almost as well as the IBA-2 model<sup>(32)</sup> with the possible exception of the stable triaxial nuclei.<sup>(33)</sup>

The relation between the two versions of the model can most readily be discussed through the introduction of  $F$  spin,<sup>(12)</sup> which is analogous to isospin for light nuclei. States with maximal  $F$  spin are fully symmetric in neutron and proton degrees of freedom. Therefore the IBA-1 model space corresponds to the subset of basis states in the IBA-2 model that have a maximal value of  $F$  spin. Since the Hamiltonian (2.10) favours states with maximal  $F$  spin the equivalence between IBA-2 and IBA-1 calculations can be understood. For a given general IBA-2 Hamiltonian an equivalent IBA-1 Hamiltonian can thus be obtained by projecting out the part that acts only on the maximal  $F$  spin subspace. The relation obtained for the parameters of the two versions of the model can be written as<sup>(32)</sup>

$$\begin{aligned} \kappa &= \kappa_{v\pi} N_v N_\pi / N(N-1) \\ \chi &= (\chi_v + \chi_\pi) / 2 \\ \kappa' &= (C_0 - 5C_2 + 54C_4) / 450 \\ \kappa'' &= (7C_2 - 2C_0 + 18\kappa') / 84 \\ \kappa''' &= 7(C_4 - 8\kappa' - \kappa'') \\ \varepsilon &= \varepsilon_{v\pi} + (4 - \chi^2)\kappa - 6\kappa' - 7\kappa'' - 9\kappa''' \end{aligned} \quad (2.12)$$

where, to shorten notation, we have, introduced

$$\begin{aligned} C_0 &= P_\nu C_\nu^0 + P_\pi C_\pi^0 - 2B \\ C_2 &= P_\nu C_\nu^2 + P_\pi C_\pi^2 + 3B/7 \\ C_4 &= P_\nu C_\nu^4 + P_\pi C_\pi^4 - 4B/7 \end{aligned}$$

with  $B = \kappa(\chi^2 - \chi_\nu \chi_\pi)$  and  $P_\rho = N_\rho(N_\rho - 1)/N(N - 1)$ ;  $\rho = \nu, \pi$ . The total number of bosons in the IBA-1 model calculation is taken as  $N = N_\nu + N_\pi$ . It has been shown that for most realistic cases the energies calculated with the full IBA-2 Hamiltonian and those with the projected Hamiltonian give almost the same results for low-lying states.<sup>(32)</sup> In some cases the agreement can be improved by minor adjustments of  $\kappa$  and  $\varepsilon$ .

### 3. MICROSCOPIC FORMULATION: ODD-MASS NUCLEI

#### 3.1. Definition of the model basis space

The IBA model can be extended to include the description of odd-mass nuclei by introducing explicitly single particle (s.p.) degrees of freedom. In the Interacting Boson Fermion Approximation (IBFA) model<sup>(17)</sup> an odd-nucleon creation operator  $a_j^\dagger$  is introduced in addition to the  $s$ - and  $d$ -boson operators. The states in the IBFA model space can, as in the case of the IBA model, be related to a shell-model basis by using the GS scheme. In order to construct an orthogonal basis, the odd-nucleon operator  $a_j^\dagger$  should not be regarded as a nucleon creation operator in the shell-model sense but rather as a generalized seniority raising operator,<sup>(32)</sup>

$$a_j^\dagger |s^N\rangle = |js^N\rangle \leftrightarrow |n = 2N + 1, J = j, w = 1\rangle, \quad (3.1)$$

and,

$$(a_j^\dagger d^\dagger)^{(j)} |s^{N-1}\rangle = |(jd)^{(j)} s^{N-1}\rangle \leftrightarrow |n = 2N + 1, J, w = 3\rangle. \quad (3.2)$$

In general  $a_j^\dagger$  operating on an  $N$ -boson state with  $n_d$   $d$ -bosons creates a state which corresponds to a shell model state with  $n = 2N + 1$  and  $w = 2n_d + 1$ . It should be realized that for the construction of the state (3.2) in the shell model space one has to consider the component of  $D^\dagger (S^\dagger)^{N-1} |j\rangle$  orthonormal to  $S^{\dagger N} |j\rangle$ . This problem is similar to that encountered in the construction of  $w = 4$  states for even-even nuclei. Since the odd-particle operator  $a_j^\dagger$  is defined as a seniority raising operator, its matrix elements will in general be different from those of a shell-model single-nucleon creation operator  $c_j^\dagger$ . The latter has, in general, non-vanishing matrix elements with both a  $w = 1$  and a  $w = 3$  state when operating on a  $w = 2$  state,  $c_j^\dagger |w = 2\rangle = A |w = 1\rangle + B |w = 3\rangle$ , whereas the odd nucleon operator  $a_j^\dagger$  can connect a  $w = 2$  state only to a  $w = 3$  state and the matrix element with the  $w = 1$  state (by definition) vanishes,  $a_j^\dagger |w = 2\rangle = |w = 3\rangle$ . This is an important difference between the two operators  $c_j^\dagger$  and  $a_j^\dagger$  and shows one of the complications that are encountered when setting up a microscopic theory for a system that includes both bosonic and fermionic degrees of freedom. In this section we will limit ourselves to the coupling of a single odd particle to the system of bosons. Two quasi-particle systems will be dealt with in Section 4.

#### 3.2. Construction of the Quadrupole operator

Since the dominant interaction in the coupling of the odd-particle to the bosons is the neutron-proton quadrupole interaction, the first task is to construct the IBFA image of the



shell-model quadrupole operator. This problem is more complicated than the similar problem in the IBA model for even–even nuclei. This can be seen by writing the most general IBFA quadrupole operator that acts on the odd particle, including all terms not higher than second order in the  $d$ -bosons

$$Q_F^{(2)} = \sum_{j\bar{j}'} A_{j\bar{j}'} (a_j^\dagger \tilde{a}_{\bar{j}'}^{(2)}) + \sum_{j\bar{j}''k} B_{j\bar{j}''}^k [(d^\dagger s + s^\dagger \tilde{d})^{(2)} (a_j^\dagger \tilde{a}_{\bar{j}''}^{(k)})^{(2)}] + \sum_{j\bar{j}'\ell k} C_{j\bar{j}'}^{\ell k} [(d^\dagger \tilde{d})^{(\ell)} (a_j^\dagger \tilde{a}_{\bar{j}'}^{(k)})^{(2)}]. \quad (3.3)$$

Whereas in the IBA model the quadrupole operator  $Q_B$  (2.7) contains only two parameters, there are up to 25 parameters to be determined in the operator (3.3), even for the simple case of a particle in a single- $j$  orbit. The main goal of the microscopic theories presented here is to arrive at a simplified expression for the quadrupole operator with a minimum of free parameters.

### 3.2.1. Direct mapping

The approach taken by Talmi, in Ref. 34, focuses on the determination of the structure of the quadrupole operator in the IBFA space rather than on the  $N$  dependence of the parameters. The method used is very similar to the one that has been used for even–even nuclei, namely matrix elements are equated for lowest seniority states. (In Ref. 34 only a three-particle system has been considered but recently the approach has been generalized to a many particle system.<sup>(35)</sup>)

A general nucleon-pair operator can be defined as

$$B_{JM}^\dagger = \sum \beta_{j\bar{j}'}^J (c_j^\dagger c_{\bar{j}'}^\dagger)_M^{(J)}, \quad (3.4)$$

which for  $J = 0$  corresponds to the  $S$  pair operator and for  $J = 2$  to the  $D$  pair creation operator. The operators  $c_j^\dagger$  are the shell-model single-nucleon creation operators. The matrix elements of the shell-model quadrupole operator  $q^{(2)}$  (eqn. 2.5) for a three-particle state can be calculated using the fermion commutation rules. For each of the components of the operator we can write,

$$\begin{aligned} \langle 0 | B_{J_1 M_1} c_{j_1 m_1} c_{\bar{j}_1 m_1}^\dagger \tilde{c}_{j_2 m_2} c_{\bar{j}_2 m_2}^\dagger B_{J_2 M_2}^\dagger | 0 \rangle &= \langle 0 | B_{J_1 M_1} B_{J_2 M_2}^\dagger | 0 \rangle \delta_{j_1 j_2} \delta_{m_1 m_2} \delta_{\bar{j}_1 \bar{j}_2} \delta_{m_1 m_2} \\ &+ \langle 0 | B_{J_1 M_1} c_{j_1 m_1}^\dagger c_{\bar{j}_1 m_1} B_{J_2 M_2}^\dagger | 0 \rangle \delta_{j_1 j_2} \delta_{m_1 m_2} - \langle 0 | B_{J_1 M_1} c_{j_2 m_2}^\dagger c_{\bar{j}_2 m_2} B_{J_2 M_2}^\dagger | 0 \rangle \delta_{j_1 j_2} \delta_{m_1 m_2} \\ &- \langle 0 | B_{J_1 M_1} c_{j_1 m_1}^\dagger c_{\bar{j}_1 m_1} B_{J_2 M_2}^\dagger | 0 \rangle \delta_{j_1 j_2} \delta_{m_1 m_2} - \langle 0 | B_{J_1 M_1} c_{j_2 m_2}^\dagger c_{\bar{j}_2 m_2}^\dagger c_{j_1 m_1} c_{\bar{j}_1 m_1} B_{J_2 M_2}^\dagger | 0 \rangle. \end{aligned} \quad (3.5)$$

In (3.5) the first term gives rise to a pure single-fermion quadrupole operator while the second term contributes only to a pure boson quadrupole operator and neither will be considered any further. The last three terms represent the corrections to the quadrupole operator coming from the Pauli principle.

Using the definition (3.4) for the pair operators, the matrix elements of the quadrupole operator  $\sum (c_j^\dagger c_{\bar{j}'}^\dagger)_k^{(k)} Q_{j\bar{j}'}$  can be calculated. Keeping only the terms that correspond to the contractions implied by the last three terms of eqn. (3.5) we obtain

$$\begin{aligned} &-4(-1)^{j_1 - m_1} Q_{j_1 \bar{j}_1} \begin{pmatrix} j_1 & k & j_1 \\ -m_1 & \kappa & m_1 \end{pmatrix} \beta_{j_1 \bar{j}_1}^{j_1} \beta_{j_1 \bar{j}_1}^{j_1} (j_2 m_2 j' m' | j_2 j' J_1 M_1) (j' m' j'' m'' | j' j'' J_2 M_2) \\ &-4(-1)^{j_2 - m_2} Q_{j_2 \bar{j}_2} \begin{pmatrix} j_2 & k & j_2 \\ -m_2 & \kappa & m_2 \end{pmatrix} \beta_{j_2 \bar{j}_2}^{j_2} \beta_{j_2 \bar{j}_2}^{j_2} (j \mu j'' m'' | j j'' J_1 M_1) (j_1 m_1 j'' m'' | j_1 j'' J_2 M_2) \\ &-4(-1)^{j_1 - m_1} Q_{j_1 \bar{j}_1} \begin{pmatrix} j_1 & k & j_1 \\ -m_1 & \kappa & m_1 \end{pmatrix} \beta_{j_1 \bar{j}_1}^{j_1} \beta_{j_1 \bar{j}_1}^{j_1} (j \mu j_2 m_2 | j j_2 J_1 M_1) (j' m' j_1 m_1 | j' j_1 J_2 M_2) \end{aligned} \quad (3.6)$$

where a summation over repeated indices is assumed. It should be noted that (3.6) contains only the contribution that will map onto a real mixed boson–fermion quadrupole operator.

In the IBFA model space an operator can be constructed of the kind (3.3) for which the matrix elements between the IBFA states are equal to those for the equivalent shell model states (3.6),

$$\begin{aligned}
 Q_F^{(2)} = \sum_{j'j''} 4 \sqrt{\frac{(2J_1+1)(2J_2+1)}{(2j+1)(2j'+1)}} & \{ Q_{j_1j''} \beta_{j_2j''}^{j_1} B_{j_2j''}^{j_1} ([a_{j''}^\dagger (b_{j_1}^\dagger \tilde{a}_{j_2})^{j'} \tilde{b}_{j_2}]^{j'})^{(2)} \\
 & - Q_{j_1j''} \beta_{j_2j''}^{j_1} \beta_{j_1j''}^{j_2} ([b_{j_1}^\dagger (\tilde{b}_{j_2} a_{j_1}^\dagger)^{j'}]^{j'} \tilde{a}_{j_2})^{(2)} \\
 & - Q_{j_1j''} \beta_{j_2j''}^{j_1} \beta_{j_1j''}^{j_2} : ([\tilde{b}_{j_2} a_{j_1}^\dagger]^{j'} [b_{j_1}^\dagger \tilde{a}_{j_2}]^{j'})^{(2)} : \}. \tag{3.7}
 \end{aligned}$$

The three terms in (3.7) correspond to the three terms in (3.6) in the same order.

The symbol  $(: \cdot :)$  indicates normal ordering, terms arising from commuting the operators in this expression should be discarded. The boson operators  $b_j^\dagger$  correspond to  $s^\dagger$  for  $J = 0$  and to  $d^\dagger$  for  $J = 2$  respectively. Similarly the coefficients  $\beta_{jj'}^j$  are related to  $\beta_{jj'}$  as introduced in eqn. (2.3) and to  $\alpha_j$ , defined in eqn. (2.1), depending on the value of  $J$ . The operator (3.7) represents a special choice of the general quadrupole operator (3.3). In principle the coefficients  $\beta_{jj'}^j$  follow from a microscopic calculation<sup>(15,16,21,31,36-38)</sup> of the structure of the fermion pair states. In this case the IBFA image of the quadrupole operator is completely determined to lowest order in the  $d$ -boson operators. The  $N$  dependence of the coefficients can be obtained in a similar approach.<sup>(35)</sup>

3.2.2. Nuclear field theory

The matrix elements of the quadrupole operator can also be derived in a Nuclear Field Theory (NFT) approach.<sup>(39)</sup> Here the approach taken by Vitturi<sup>(40)</sup> will be described. The NFT provides diagrammatic rules to calculate perturbative matrix elements between collective states. The small parameter in this perturbation series is  $1/\Omega$ ,  $\Omega = (2j + 1)/2$  being the pair degeneracy of the shell. Terms which are higher order in  $1/\Omega$  correspond in general to higher order terms in the collective boson degrees of freedom. The leading order terms give rise to the one-body terms while the terms of the order  $1/\Omega$  contribute to a two-boson or a boson-fermion operator.

In Fig. 2 the lowest order additional graphs that contribute to the matrix elements of the

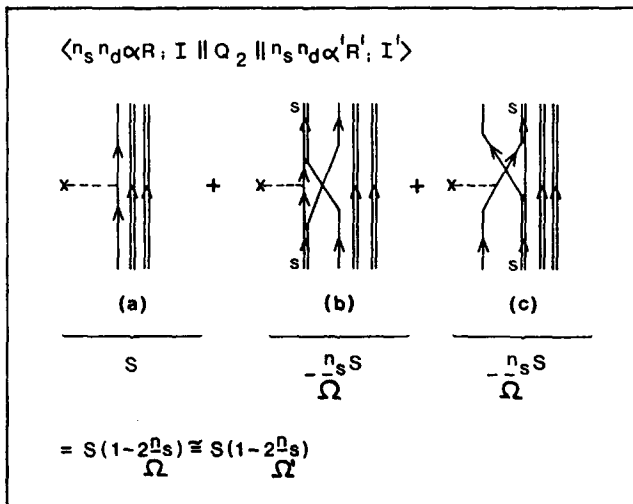


Fig. 2. Diagrams in NFT that contribute to the matrix elements of the quadrupole operator (after Ref. 40).

quadrupole operator due to the presence of the odd particle are shown. Graph (a) corresponds to the zero order contribution in which the quadrupole field acts on the odd particle without any interaction with the bosons. The other two terms give rise to corrections of the order of  $1/\Omega'$ , where<sup>(40,41)</sup>  $\Omega' = \Omega - 2n_d - 1$ . The total contribution to order  $1/\Omega'$  to the matrix element is given by<sup>(40)</sup>

$$\langle n_s n_d \alpha R; j J \| Q \| n_s n_d \alpha' R'; j J' \rangle = S \left( 1 - \frac{2n_s}{\Omega'} \right)$$

for the case of a single  $j$  shell, where

$$S = Q_{jj} \hat{J} \hat{J}' (-1)^{R+J} \left\{ \begin{matrix} 2 & j & j \\ R & J & J' \end{matrix} \right\} \delta_{\alpha\alpha'} \delta_{RR'}$$

The IBFA model operator can now be obtained by matching matrix elements between equivalent states resulting in

$$Q_F = \left( \frac{\Omega - 2N - 1}{\Omega'} \right) Q_{jj} (a_j^\dagger \tilde{a}_j)^{(2)}$$

where  $N$  is the total number of bosons. It is seen that some additional terms in the quadrupole operator that appear using the method described in Section 3.2.1 are not obtained. The reason is that in the present approach certain exchange diagrams have not been considered.

### 3.2.3. Quasi particles

The IBFA image of the shell model quadrupole operator can also be constructed through the introduction of pseudo particle<sup>(32)</sup> creation operators. The pseudo particle operator  $\tilde{c}_j^\dagger$  in the IBFA model is defined as the equivalent of the single-particle operator  $c_j^\dagger$  in the shell model space. The two operators are equivalent in the sense that the matrix elements of the operators between equivalent states in the two spaces are equal. It should be realized that the pseudo particle operator  $\tilde{c}_j^\dagger$  should be distinguished from the odd nucleon operator  $a_j^\dagger$  since the latter, as is remarked before, should be regarded as a seniority step operator. In order to obtain an expression for the pseudo particle operator in first order in the  $d$  boson operator, matrix elements have to be calculated in the shell-model space for states with generalized seniority  $w \leq 3$ . As an example the derivation for the  $w \leq 1$  matrix element will be outlined.

In the so-called number operator approximation (NOA), which is discussed extensively by Otsuka<sup>(16)</sup> the coefficients  $\alpha_j$  which enter in the definition of the  $S$  pair operator (2.1) are normalized such that the eigenvalue of

$$\hat{n} = \sum_j \alpha_j^2 \sum_m c_{jm}^\dagger c_{jm} = \sum_j \alpha_j^2 \hat{n}_j$$

for states with  $N-S$  pairs is equal to the number of nucleons,  $\langle S^N | \hat{n} | S^N \rangle = 2N$ . To a good approximation this operator can be treated as the number operator. In this approximation the algebra for the GS operators becomes equal to that of conventional seniority and many equations can be simplified. By introducing an effective degeneracy

$$\Omega_e = \sum_j \alpha_j^2 \Omega_j$$

of the major shell the following normalization constants can be derived,<sup>(16)</sup>

$$K_{N,0}^2 = \langle 0 | S^N S^{\dagger N} | 0 \rangle \approx N! \Gamma(\Omega_e + 1) / \Gamma(\Omega_e - N + 1),$$

$$K_{N,1}^2(j) = \langle j | S^N S^{\dagger N} | j \rangle \approx K_{N,0}^2 (1 - N\alpha_j^2 / \Omega_e)$$

for the  $S$  pair states. For later use it is convenient to introduce the occupation probabilities  $v^2 \equiv n_j/(2j+1)$ . Using

$$n_j = \langle S^N | \hat{n}_j | S^N \rangle \approx 2N\alpha_j^2\Omega_j/\Omega_e \quad (3.8)$$

these spherical shell model occupancies can be related to the structure coefficients of the  $S$ -pair state,  $\alpha_j$ , as

$$v_j^2 = \alpha_j^2 N/\Omega_e. \quad (3.9)$$

Since the spherical shell-model occupation probabilities  $v_j^2$  have a simpler physical interpretation than the coefficients  $\alpha_j$ , in the subsequent formulas all factors  $\alpha_j$  are replaced by  $v_j$  and  $u_j = (1 - v_j^2)^{1/2}$ .

The matrix elements of the shell-model creation operator between states with  $w \leq 1$  can now be calculated and equated to matrix elements of the IBFA operator,

$$\langle S^N j' \| c_j^\dagger \| S^N \rangle = -\hat{j}u_j\delta_{jj'} = u_j \langle s^N j' \| a_j^\dagger \| s^N \rangle,$$

and

$$\langle S^N \| c_j^\dagger \| S^{N-1} j' \rangle = \hat{j}v_j\delta_{jj'} = v_j \langle s^N \| (s^\dagger \tilde{a}_j)^{(j)} \| s^{N-1} j' \rangle / \sqrt{N}.$$

Similar expressions can also be obtained for  $w \leq 3$  states.<sup>(32,42)</sup> In first order in the number of  $d$ -boson operators, the IBFA image for the shell model single-nucleon creation operator can now be written as

$$\begin{aligned} c_j^\dagger = & u_j a_j^\dagger - \sum_{j'} \frac{v_j}{\sqrt{N}} \sqrt{\frac{10}{2j+1}} \beta_{j'j}(\mathbf{K}_\beta)^{-1} s^\dagger (\tilde{d}a_{j'}^\dagger)^{(j)} + \frac{v_j}{\sqrt{N}} (s^\dagger \tilde{a}_j)^{(j)} \\ & + \sum_{j'} u_j \sqrt{\frac{10}{2j+1}} \beta_{j'j}(\mathbf{K}_\beta)^{-1} (d^\dagger \tilde{a}_{j'})^{(j)}, \quad (3.10) \end{aligned}$$

where

$$K_\beta^2 = \sum_{jj'} \beta_{jj'}^2. \quad (3.11)$$

In this expression the coefficients  $\beta_{jj'}$  define the microscopic two particle structure of the  $d$ -boson [see eqn. (2.3)]. In obtaining the operator (2.7) only matrix elements between states with  $w \leq 3$  have been considered and this operator is thus only a lowest order approximation to the full image of the shell-model single-nucleon operator. Estimates of higher order contributions have not been made but it is assumed that these are small as is the case in the mapping for even-even nuclei.<sup>(16)</sup>

The coefficients  $\alpha_j$  and  $\beta_{jj'}$  can, in principle, be obtained from a microscopic calculation.<sup>(15,16,21,31,36-38)</sup> The problem can be simplified by assuming that the  $D$ -pair state exhausts the full  $E2$  sumrule strength,  $D^\dagger \sim [Q, S^\dagger]$  in which case it can be shown<sup>(32,42)</sup> that,

$$\beta_{jj'} = (u_j v_{j'} + v_j u_{j'}) Q_{jj'}, \quad (3.12)$$

where  $Q_{jj'}$  are the single particle matrix elements of the quadrupole operator. In a somewhat more sophisticated approach an energy denominator can be included<sup>(43)</sup> in eqn. (3.12) as suggested by perturbation theory. In most phenomenological applications of the IBFA model the radial matrix elements of the quadrupole operator are taken equal and are absorbed in an effective charge, which gives

$$Q_{jj'} = \langle \ell^{\frac{1}{2}} j \| Y^{(2)} \| \ell^{\frac{1}{2}} j' \rangle. \quad (3.13)$$

Using the image of the shell-model single nucleon creation and annihilation operator the boson image of the quadrupole operator can be constructed. Retaining only terms up to second order in the  $d$ -boson operators one obtains

$$Q_{BF}^{(2)} = Q_B^{(2)} + Q_F^{(2)}, \quad (3.14)$$

where

$$Q_B^{(2)} = (s^\dagger \tilde{d} + d^\dagger s)^{(2)} + \chi (d^\dagger \tilde{d})^{(2)}, \quad (3.15)$$

and

$$Q_F^{(2)} = \sum_{jj'} Q_{jj'}(u_j u_{j'} - v_j v_{j'}) (a_j^\dagger \tilde{a}_{j'})^{(2)} - (10/N)^{1/2} \times \sum_{jj'j''} Q_{jj'}(u_j v_{j'} + v_j u_{j'}) \beta_{j''j} [(d^\dagger \tilde{a}_{j'})^{(j)} (s a_{j'}^\dagger)^{(j'')}]^{(2)} (\hat{K}_\beta)^{-1}. \quad (3.16)$$

The parameter  $\chi$  which appears in eqn. (3.15) and which is important for determining the nuclear shape<sup>(44)</sup> can be expressed as

$$\chi = -10K_\beta^{-3} \sqrt{2N} \sum_{jj'j''} \beta_{j''j} \beta_{j'j''} Q_{jj'} \left\{ \begin{matrix} 2 & 2 & 2 \\ j & j' & j'' \end{matrix} \right\} (v_j v_{j'} - u_j u_{j'}). \quad (3.17)$$

The operator (3.14) can subsequently be used to construct the interaction terms in the Hamiltonian coming from the shell-model neutron–proton quadrupole interaction.

To test the accuracy of the approximation (3.16) in Ref. 27 the matrix elements of the quadrupole operator are calculated in a generalized seniority basis. In the calculation several non-degenerate orbits are considered. An explicit numerical comparison is made for all matrix elements between  $w = 1$  states and between  $w = 1$  and  $w = 3$  states for a 13 particle system with the values obtained from eqn. (3.16). Most matrix elements agree to within 10% for this realistic system in which some s.p. orbits are almost filled while others are almost empty. This clearly indicates that the simple expression (3.16) gives a good approximation of the matrix elements for the lowest seniority states.

### 3.3. The IBFA Hamiltonian

In general the IBFA Hamiltonian can be written as the sum of three terms,<sup>(17,18)</sup>

$$H = H_B + H_F + V_{BF}, \quad (3.18)$$

where  $H_B$  is the IBA Hamiltonian describing the  $s$ – $d$  boson system and  $H_F$  is the pure odd-particle part of the Hamiltonian. Since only a single odd-nucleon, which can occupy different shell model orbits  $j$ , is coupled to the system of bosons,  $H_F$  contains only one-body terms,

$$H_F = \sum_{jm} \varepsilon_j a_{jm}^\dagger a_{jm}, \quad (3.19)$$

where  $\varepsilon_j$  are the IBFA single particle energies.

In a microscopic treatment the boson–fermion interaction  $V_{BF}$  can originate from both the interaction between like particles and from the neutron–proton quadrupole–quadrupole interaction. The resulting structure of the boson–fermion interaction turns out to be identical for the two cases, but here only the latter will be considered. The interaction can be constructed using eqns. (3.14–16). The product of the two purely bosonic terms will of course give rise to a boson–boson interaction that contributes only to  $H_B$ , while the product

of  $Q_B$  and  $Q_F$  contributes to  $V_{BF}$ . Furthermore in the IBFA-1 model neutron and proton boson degrees of freedom are not distinguished. The boson–fermion interaction obtained in the way described above should, therefore, be mapped from a neutron–proton basis onto a one-kind of boson basis. The two model bases can be related by introducing  $F$ -spin, as was discussed in Section 2.4. Since in  $Q_{BF}$  only terms up to second order in the  $d$ -boson operators have been considered, no terms higher than second order in these operators will be included in  $V_{BF}$ . The interaction can now be written as,<sup>(17,32,42)</sup>

$$V_{BF} = \sum_j A_j \hat{n}_d \hat{n}_j + \sum_{jj'} \Gamma_{jj'} (Q_B^{(2)} \cdot (a_j^\dagger \tilde{a}_j)^{(2)}) + \sum_{jjj''} \Lambda_{jjj''} : ((d^\dagger \tilde{a}_j)^{(j'')} \times (\tilde{d} a_j^\dagger)^{(j'')})_0^{(0)} : \frac{1}{j''}. \quad (3.20)$$

The first term is the monopole interaction, which has the effect of changing the  $d$ -boson energy. In most phenomenological applications the strength of the monopole force has been taken as constant,  $A_j = A_0$  and is such that it hardly affects the structure of the spectrum. The product of the boson quadrupole operator with the pure fermion part of (3.14) gives rise to the second term in (3.20), the boson–fermion quadrupole interaction. The mixed term in (3.14) which arises from the fact that the bosons are built up from fermions occupying the same orbits as the odd fermion gives rise to the third term in (3.20). It arises from the action of the Pauli principle between the bosons and the odd fermion and is therefore referred to as the exchange interaction. We note that a similar form for the exchange force can also be derived assuming a quadrupole pairing interaction between like bosons.

The above microscopic arguments also dictate a certain  $j$ -dependence of the parameters  $\Gamma$  and  $\Lambda$ ,

$$\Gamma_{jj'} = \Gamma_0 (u_j u_{j'} - v_j v_{j'}) Q_{jj'}, \quad (3.22)$$

$$\Lambda_{jjj''} = -2\sqrt{5} \Lambda_0 \beta_{jj'} \beta_{j''}, \quad (3.23)$$

where  $u_j$ ,  $v_j$ , and  $\beta_{jj'}$  are defined in eqns. (3.9 and 3.12). The projection from a neutron–proton basis to a maximal  $F$ -spin basis introduces an explicit  $N$ -dependence in the parameters (for a proton odd fermion)

$$\Gamma_0 = \bar{\kappa} N_v / (N_v + N_\pi), \quad (3.24)$$

$$\Lambda_0 = \bar{\kappa} \frac{1}{K_\beta} N_v \sqrt{10 N_\pi} / (N_v + N_\pi), \quad (3.25)$$

$$\kappa = -\bar{\kappa} K_\beta / \sqrt{2 N_\pi}. \quad (3.26)$$

The constant  $K_\beta$  is defined in eqn. (3.11),  $\bar{\kappa}$  is related to the basic shell-model neutron–proton interaction and  $\kappa$  is the strength of the quadrupole force in the IBA-2 model.

### 3.4. Relation to other quasi-particle-core coupling models

Odd-mass nuclei have been extensively described in terms of quasi-particle-core coupling models.<sup>(45)</sup> The coupling of the q.p. to the core is conventionally described by a quadrupole–quadrupole force, which is similar in nature to the quadrupole term in the boson–fermion interaction. The dependence of the strength on the occupancies of the orbits involved has also been derived in a BCS framework and the results are identical to that which has been derived for the IBFA model.

Only much after the development of the quasi-particle core coupling models was it realized that the pure quadrupole coupling did not describe the complete picture. In 1966 Kisslinger<sup>(46)</sup> showed the importance of including three quasi-particle states in the q.p.-core

coupling basis in order to be able to explain the so-called  $J = j - 1$  anomaly. It was shown that the diagonal matrix elements of the quadrupole interaction for the anti-symmetrized three q.p. states were given by

$$V_{jj}^J = \frac{2}{3}\kappa Q_{jj}(u_j v_j)^2 [1 - 10 W(2jj2; jJ)] \tag{3.27}$$

where  $\kappa$  is the strength of the quadrupole–quadrupole interaction and  $W$  is the Wigner 6- $j$  symbol. Also in an extension of the quasi-particle random phase approximation one obtains a similar expression only as a result of the inclusion of three q.p. states in the basis.<sup>(47)</sup> This expression is identical to eqn. (4.4) which gives the energy splitting of the one  $d$  boson quintuplet in IBFA under the influence of the exchange force. In the IBFA model one therefore does not have to introduce additional q.p. degrees of freedom. The splitting arises naturally from the action of the Pauli principle between the odd fermion and the fermions that form the bosons in a microscopic treatment of the IBFA model. The origin of the exchange force can also be understood from a pure shell model formulation as the result of the interaction between like particles. The matrix elements of a rank 2 tensor interaction (quadrupole pairing for example) can be calculated analytically<sup>(28)</sup> for a  $j^n, v = 3$  state, and one obtains an expression for the energies which is similar to eqn. (4.4).

In an approach based on RPA Dönau and Hagemann<sup>(48)</sup> have also introduced a formulation for the boson–fermion interaction. Even though their philosophy differs from that of the IBA model, the interaction obtained is for all practical purposes identical to that of the IBFA model.

From the similarities between the different models in the formulation of the particle core interaction it is evident that in applications to spherical nuclei all these models will give similar results. It is, however, not possible to extend the q.p. core coupling models, with the exception of the model of Refs 48 and 49, to the case of deformed nuclei. As is shown in the next section, it is possible in the IBFA model to describe both spherical and deformed nuclei using a single formulation of the boson–fermion interaction.

## 4. PHENOMENOLOGY

### 4.1. Geometrical limits

The geometrical limits of the IBFA model can best be discussed in terms of schematic calculations in the various limits of the IBA-core Hamiltonian. Using the simplified case in which the odd particle occupies a single  $j$ -orbit it will be shown that in the  $SU(5)$  limit the particle vibration coupling scheme is reproduced, in the  $SU(3)$  limit the Nilsson scheme, while in the  $O(6)$  limit that of a particle coupled to a classical gamma unstable rotor. These examples correspond to realistic cases in which a unique parity orbit is coupled to the bosons. In this special case of a single- $j$  orbit the general boson–fermion interaction (3.20) can be simplified to

$$V_{BF} = \Gamma_{jj} Q_B^{(2)} \cdot (a_j^\dagger \hat{a}_j)^{(2)} + \Lambda_{jj}^j : [(\tilde{d} a_j^\dagger)^{(j)} \times (d^\dagger \tilde{a}_j)^{(j)}]^{(0)} : \hat{j}^{-1} \tag{4.1}$$

where the monopole interaction has been omitted. For the following discussion it is more transparent to relate the two parameters in (4.1) directly to the occupancy  $v_j^2$  of the orbit, using eqns. (3.22) and (3.23),

$$\begin{aligned} \Gamma_{jj} &= \Gamma_0 (u_j^2 - v_j^2) Q_{jj} \\ \Lambda_{jj}^j &= -8\sqrt{5} \Lambda_0 u_j^2 v_j^2 Q_{jj} Q_{jj} \end{aligned} \tag{4.2}$$

For each of the three limits of the IBA model<sup>(2,3,4)</sup> the IBFA results will be presented as a function of the occupancy  $v_j^2$  of the s.p. orbit.

4.1.1. *The SU(5) limit*

The  $SU(5)$  limit is obtained in the IBA Hamiltonian by taking  $\varepsilon$ , the  $d$ -boson energy, much larger than the strength  $\kappa$  of the boson quadrupole interaction. Since the strength of the boson-boson and the boson-fermion interactions are related, in this case also  $\varepsilon$  will be large compared to the boson-fermion interaction. The weak coupling scheme should thus provide the appropriate coupling scheme for the wave functions,

$$|\alpha, L, j, J\rangle = \{|\alpha, L\rangle \otimes |j\rangle\}^{(J)}. \tag{4.3}$$

The quantum numbers necessary to uniquely label the core state are  $\alpha = \{N, n_d, v, n_\delta\}$ . The  $J_z$  quantum number has been suppressed.

In the basis (4.3) the matrix elements of the boson-fermion interaction (4.1) can be calculated analytically.<sup>(3,2)</sup> The result obtained for the quintuplet of states with  $n_d = 1$  can be expressed as

$$\langle n_d = 1, L = 2, j, J | V_{BF} | n_d = 1, L = 2, j, J \rangle = 5\Gamma_{jj}(-1)^{j-j} \left\{ \begin{matrix} 2 & 2 & 2 \\ j & j & j \end{matrix} \right\} + \Lambda_{jj}^j \left\{ \begin{matrix} 2 & j & j \\ 2 & j & j \end{matrix} \right\}. \tag{4.4}$$

In Fig. 3 the calculated spectra, using the computer code 'ODDA',<sup>(50)</sup> are shown as a function of  $v_j^2$  for the case that  $j = 9/2$ . The parameters  $\varepsilon = 0.7$ ,  $\Gamma_0 = 0.567$  and  $\Lambda_0 = 1.83$  have been given realistic values. The parameter  $\chi$  has been given the  $SU(3)$  value,  $\chi = -\frac{1}{2}\sqrt{7}$ . Recent investigations<sup>(100)</sup> suggest that half this value is more realistic, but for the present purpose this difference is irrelevant. For the cases where  $v^2 = 0$  or  $v^2 = 1$  the odd particle is coupled to the core by a pure quadrupole force with opposite sign for the two

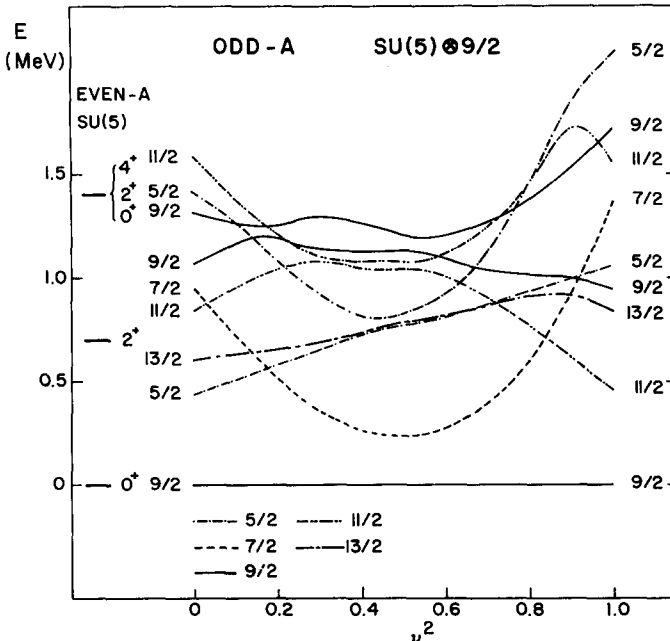


Fig. 3. Calculated low-lying states for the system of a  $j = 9/2$  particle coupled to  $SU(5)$  ( $N = 5, \varepsilon = 0.7$  in (2.11)) as a function of  $v_j^2$  using eqns. (4.1) and (4.2) with  $\Gamma_0 = 0.567$  MeV,  $\Lambda_0 = 1.83$  MeV,  $\chi = -1/2\sqrt{7}$ .



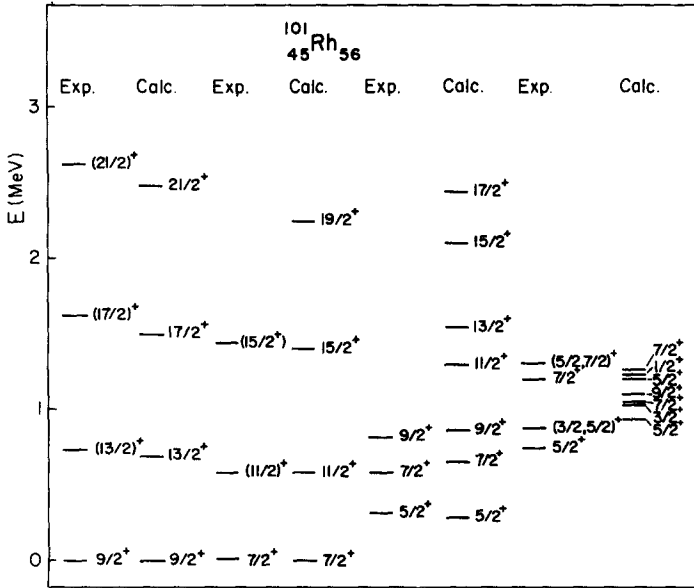


Fig. 4. Calculated and experimental low-lying positive parity levels in  $^{101}_{45}\text{Rh}_{56}$ . In the calculation a  $g_{9/2}$  proton is coupled to  $^{100}_{44}\text{Ru}_{56}$  via a pure exchange force,  $v_j^2 = 0.5$ ,  $\Lambda_0 = 2.32$  MeV. The core parameters<sup>(2)</sup> were taken from a best fit,  $\epsilon = 0.733$  MeV,  $c_L = -0.415, -0.283, -0.024$  MeV,  $v_2 = 1.75$  MeV,  $v_0 = -0.32$  MeV.<sup>(2)</sup>

cases. Due to the fact that the quadrupole coupling also gives rise to mixing of multiplets with different values of  $n_d$ , the splitting of the levels in the quintuplet are not exactly opposite to each other for the two limits. In the case that  $v^2 = 0.5$  the ordering of the levels is completely different. The fact that in this case the state with  $J = j - 1$  is by far the lowest member of the quintuplet follows directly from eqn. (4.4) if the values for the six- $j$  symbols are substituted. This  $J = j - 1$  anomaly is known to occur in the shell model as a result of the Pauli principle. In the IBFA model it is due to the exchange force which, as is clear from the microscopic derivation, takes into account the effects of the Pauli principle between the odd particle and the bosons.

As an example of the  $J = j - 1$  anomaly in Fig. 4 the spectrum of  $^{101}\text{Rh}$  ( $Z = 45$ ) is shown. This nucleus has been calculated<sup>(32)</sup> by coupling a particle in the  $g_{9/2}$  shell to a  $^{100}_{44}\text{Ru}$  core. For  $Z = 45$  one expects the  $g_{9/2}$  orbit to be half filled,  $v^2 = 0.5$  and in the calculation therefore, only the exchange force has been considered in  $V_{BF}$ .

#### 4.1.2. The SU(3) limit

For the case of a particle coupled to a  $SU(3)$  core the weak coupling basis is no longer applicable, but instead a strong coupling basis has to be introduced,<sup>(32)</sup>

$$|N, (\lambda, \mu), K_c; jK_j; KJM\rangle = \sum_R \sqrt{(1 + \delta_{K_c, 0})} \hat{R} \left( \begin{matrix} j & R \\ K_{j\pm} & K_c - j \end{matrix} \right) \{ |N(\lambda, \mu)K_c R\rangle \times |j\rangle \}_M^{(j)}. \quad (4.5)$$

The core states are labeled by  $N$ , the total number of bosons, by  $(\lambda, \mu)K_c$  which label the  $SU(3)$  representation and  $R$ , the spin of the core state. In a geometrical description the  $K$ -quantum number corresponds to the projection of the angular momentum on the symmetry axis. Only in the limit of large  $N$  the states (4.5) are eigenstates of the Hamiltonian. Since in realistic cases the  $SU(3)$  limit only occurs if  $N$  is large this is not causing any

severe restrictions. The asymptotic wave functions (4.5) will prove to be sufficiently accurate to discuss the features of the IBFA Hamiltonian.

In the limit of large  $N$  the matrix elements of the interaction can be calculated in the basis (4.6) using<sup>(32)</sup>

$$\lim_{\substack{\lambda \rightarrow \infty \\ \lambda \gg \mu}} \langle N, (\lambda, \mu) K_c R \parallel (d^\dagger \bar{d})^{(L)} \parallel N, (\lambda', \mu'), K'_c R' \rangle / \lambda \\ = (-1)^{R-K_c} 1/3 \hat{L} \hat{R} \hat{R}' \begin{pmatrix} R & R' & L \\ K_c & -K'_c & 0 \end{pmatrix} \begin{pmatrix} 2 & 2 & L \\ 0 & 0 & 0 \end{pmatrix} \delta_{\lambda\lambda'} \delta_{\mu\mu'} \delta_{K_c K'_c}, \quad (4.7)$$

and

$$\lim_{\substack{\lambda \rightarrow \infty \\ \lambda \gg \mu}} \langle N, (\lambda, \mu) K_c R \parallel (s^\dagger \bar{d} + d^\dagger s)^{(2)} \parallel N, (\lambda', \mu'), K'_c R' \rangle / \lambda \\ = (-1)^{R-K_c} \frac{2\sqrt{2}}{3} \hat{R} \hat{R}' \begin{pmatrix} R & R' & 2 \\ K_c & -K'_c & 0 \end{pmatrix} \delta_{\lambda\lambda'} \delta_{\mu\mu'} \delta_{K_c K'_c}. \quad (4.8)$$

Note that in this limit all non-diagonal matrix elements vanish and only even values of  $L$  contribute to (4.7). The matrix elements of the interaction now follow trivially. In the case  $j = j' = j''$  they read

$$\lim_{\substack{\lambda \rightarrow \infty \\ \lambda \gg \mu}} \langle N, (\lambda, \mu), K_c; j K_j; K \mid V_{BF} \mid N, (\lambda, \mu) K_c; j K_j; K \rangle / \lambda \\ = -\Gamma_{jj} \sqrt{5/2} R_j(K_j) - \Lambda_{jj}^j R_j^2(K_j) / 3 \quad (4.9)$$

where

$$R_j(K) = [3K^2 - j(j+1)] / \sqrt{(2j-1)j(2j+1)(j+1)(2j+3)}. \quad (4.10)$$

In this example the  $SU(3)$  quadrupole operator [eqn. (2.11)] has been taken with  $\chi = -\frac{1}{2}\sqrt{7}$ . It is important to notice that the two terms in the interaction (4.1) give rise to a different  $K$ -dependence. In the presence of only the quadrupole force the energies of the bandheads depend linearly on  $K_j^2$ . Depending on whether the shell is filled or not one expects the bands to be ordered according to increasing or decreasing values of  $K_j$ . For an empty orbit,  $v^2 = 0$ , coupled to a prolate deformation the  $K_j = 1/2$  forms the ground state band while for  $v^2 = 1$  this will be the  $K_j = j$  band. As an example in Fig. 5 a calculated spectrum is shown in the latter limit. The spectrum is arranged in several rotational bands in which the energies are proportional to  $J(J+1)$ . For low values of  $K_j$ , especially  $K_j = 1/2$ , this level sequence is considerably perturbed. In the Nilsson model this is known to be due to the effects of the Coriolis force which for a  $K = 1/2$  band is the origin of the well known signature splitting. As is the case in the rotational model, the sign of the signature splitting is given by  $(-1)^{j-1/2}$ . In the IBFA model the equivalent of Coriolis mixing comes in part from the finite value of the moment of inertia of the core and in part from off-diagonal matrix elements of the interaction in the strong coupling basis (4.5) due to a finite value of  $N$ . In Fig. 5 additional bands are predicted at an energy of about 1 MeV above the bandhead. These correspond to the coupling of the particle to the so called  $\beta$  and  $\gamma$  bands of the core.

In the case where a particle is coupled to the rotor only via the exchange force a different picture emerges (see Fig. 6). As can be seen from eqn. (4.2) in this case the shell  $j$  is only half filled in the spherical limit. In the Nilsson scheme<sup>(51)</sup> one would expect, therefore, to have all deformed orbits up to  $K_j = j/2$  filled while the higher ones are empty and thus have the  $K_j = j/2$  as a ground state band. The same picture emerges in the IBA model since for the case that  $\Gamma_{jj} = 0$  and  $\Lambda_{jj}^j < 0$ , the groundstate band will have a value of  $K$  for which  $R_j^2(K_j)$  is minimal, i.e.  $K_j = \sqrt{j(j+1)/3} \simeq j/2$ .

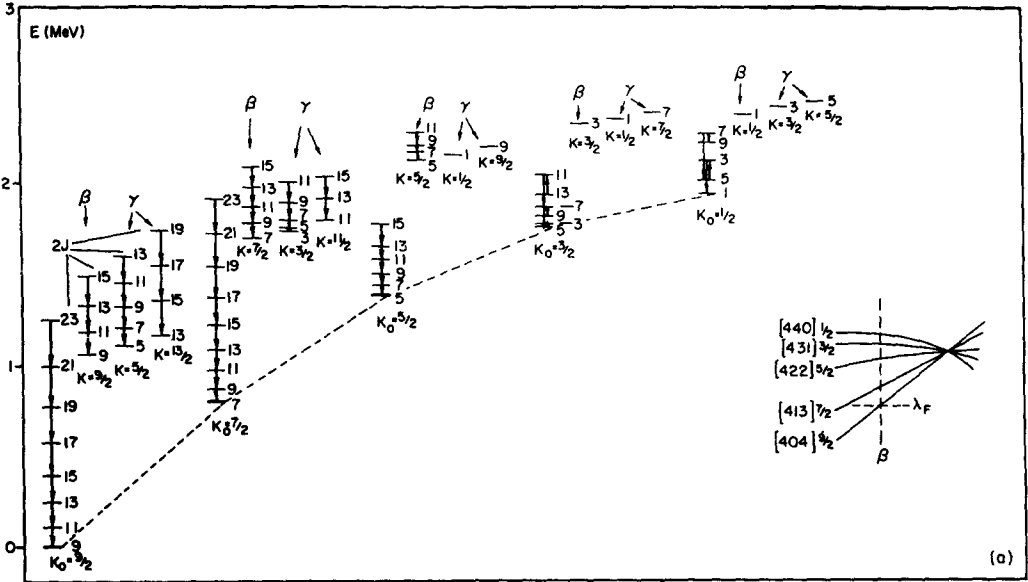


Fig. 5. A typical spectrum in the  $SU(3)$  limit of the interacting boson-fermion model. The  $SU(3)$  core is described by (2.11) with  $N = 6, \kappa = 12.5$  keV. A  $j = 9/2$  particle is coupled to this core via a pure quadrupole force,  $v_j^2 = 1, \Gamma_0 = 0.23$  MeV,  $\chi = -1/2\sqrt{7}$  in eqns. (4.1) and (4.2). Only a selected number of levels is shown. In the inset the corresponding situation in the Nilsson model is shown.

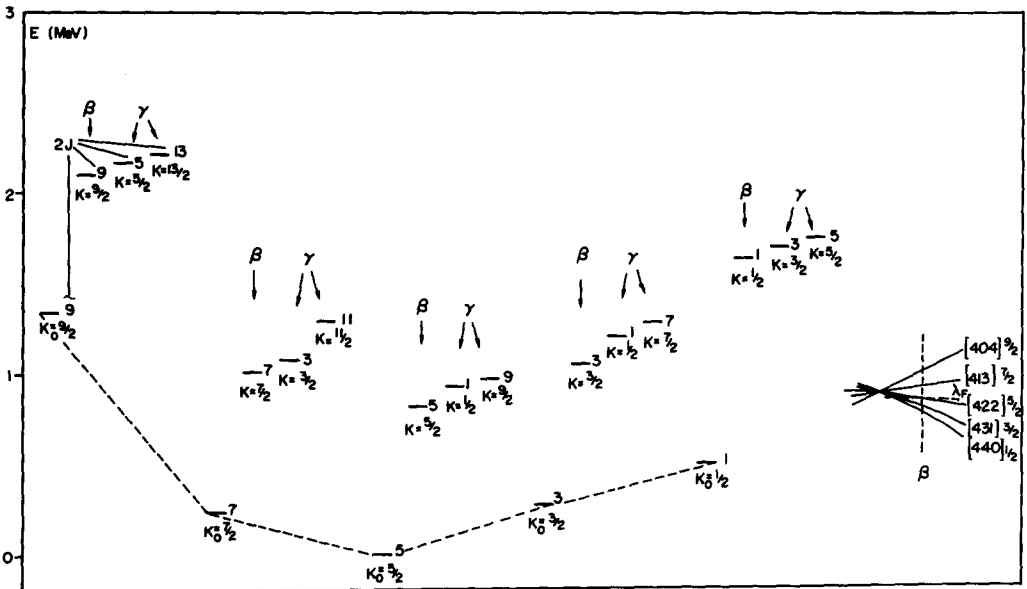


Fig. 6. Same as Fig. 5, but for  $v^2 = 0.35, \Gamma_0 = 0.23$  MeV,  $\Lambda = 1.12$  MeV,  $\chi = -1/2\sqrt{7}$ . Only the lowest state of each band is shown.

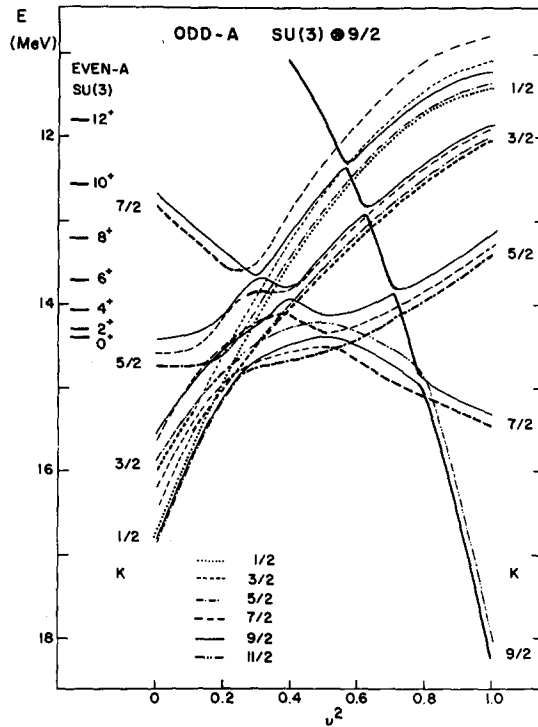


Fig. 7. Calculated levels for the system of a  $j = 9/2$  particle coupled to an  $SU(3)$ -core ( $N = 9$ ,  $\kappa = 50$  keV,  $\kappa' = 20.8$  keV in eqn. (2.11) as a function of  $v_j^2$  using eqns. (6.2)–(6.6) with  $\Gamma_0 = 0.567$  MeV,  $\Lambda_0 = 1.83$  MeV and  $\chi = -1/2\sqrt{7}$ . The bandheads are indicated by a heavy line.

On top of each of the bandheads a rotational band is built. Due to the fact that the bandheads are relatively close, the Coriolis mixing is much larger than was the case in Fig. 5. Therefore, in order to avoid confusion in Fig. 6, only the positions of the bandheads are indicated.

To show even more clearly the close relation between the Nilsson scheme and the IBFA model for an axially deformed nucleus, the bands related to the  $(\lambda, \mu) = (2N, 0)$   $SU(3)$  configuration are plotted in Fig. 7 as a function of the occupancy of the spherical s.p. orbit. In the Nilsson model one expects that by increasing the occupancy the  $K$ -value of the groundstate band increases as a result of the rising of the Fermi energy. The same picture emerges in the IBFA model. For small values of  $v_j^2$  the Coriolis force strongly breaks the band structure of the  $K = 1/2$  and  $K = 3/2$  bands. For  $v_j^2 > 0.3$  the groundstate band is well developed and for increasing values of  $v_j^2$  the  $K$  value of the groundstate band varies like it does in the Nilsson model.

The relation between the  $SU(3)$  limit in the IBFA model and a geometrical rotor is even more apparent if some of the more detailed predictions of the two models are compared. Recently Hamamoto<sup>(52)</sup> has brought to attention some remarkable properties of electromagnetic transitions in the geometrical model which, as shown by Frauendorf and Dänau,<sup>(53)</sup> can be explained by signature splitting as a result of the strong perturbative effect of the rotation. Calculations, which for simplicity have been limited to a unique parity orbit  $j = 13/2$ , were performed<sup>(52)</sup> in the cranking model and a particle-rotor model using BCS

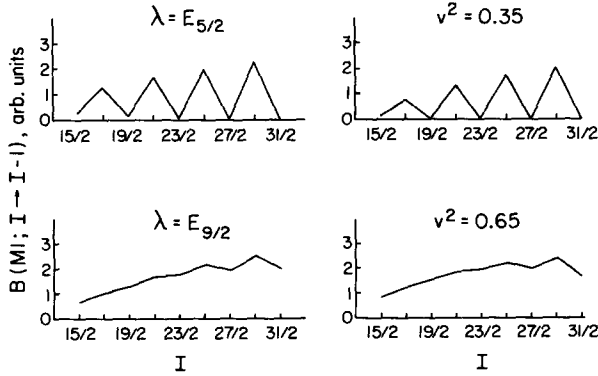


Fig. 8. Calculated  $M1$  transition probabilities between Yrast states. The coupling of an  $i_{13/2}$  particle to a deformed core is described in a geometrical picture (left) and the IBFA model (right). The parameters used in the IBFA particle-core coupling are  $\Gamma_0 = 0.5$  MeV and  $\Lambda_0 = 1.5$  MeV. The core is described by  $N = 8$ ,  $\kappa = +0.015$  MeV and  $\kappa' = -0.004$  MeV [see eqn. (2.11)]. In the two geometrical model calculations<sup>(52)</sup> the Fermi level is placed on the  $\Omega = 5/2$  and  $\Omega = 9/2$  single particle energies of the intrinsic Hamiltonian. In the IBFA the corresponding spherical shell model occupancies have been chosen.

one quasi-particle states. Two different values for the Fermi energy were taken, equal to the energies of the s.p. states of the intrinsic Hamiltonian with  $K = 5/2$  and  $9/2$ . The calculated pattern<sup>(52)</sup> for the  $M1$  transitions is shown in Fig. 8. The  $B(M1; I \rightarrow I-1)$  values for  $I = j+2n$  where  $n$  is an integer are much larger than those for  $I = j+2n+1$ . The  $B(M1; I \rightarrow I-1)$  vanishes for  $I = j+2n+1$  when the  $|I-1\rangle$  and  $|I-2\rangle$  levels or the  $|I+1\rangle$  and  $|I\rangle$  levels are degenerate in energy. Since this situation is reached only for low values of  $K$ , the effect is stronger for  $K = 5/2$  than for  $K = 9/2$  as is clear from Fig. 8.

The same effect is also observed in the IBFA model. In Fig. 8 the  $B(M1)$  values in the groundstate band are also plotted, calculated in the IBFA model for two cases, one in which  $v^2$  is chosen such as to have a  $K = 5/2$  groundstate band and one in which the groundstate band is  $K = 9/2$ . The parameters in the  $M1$  transition operator [Eqns. (4.12–4.14)] are taken as  $g_d = 0.0$  n.m.,  $g = 1.0$  n.m. and  $g_s = 4.0$  n.m. but the calculated phenomena are essentially independent of the choice of the  $M1$  operator. As is clear, exactly the same features are observed, even to the extent that the  $M1$  transitions vanish whenever degeneracies occur in the spectrum. The degeneracies suggest a picture in which the two levels of the doublet can be characterized by an intrinsic angular momentum  $L = j-1/2+2n$  to which a spin  $1/2$  is coupled. The selection rule for the  $M1$  transitions is thus automatically explained. In the calculation presented in Ref. 52 it is shown that also in the rotational model the  $B(E2)$  transitions show an enhancement of up to a factor 2 for  $\Delta J = 2$  transitions relative to  $\Delta J = 1$  transitions in a band. This particular feature is also reproduced in the IBFA calculations reported above.

The most important result of this comparison of these two, conceptually completely different, models is that not only basic features, such as the dependence of the  $K$ -value of the groundstate band on the occupancy of the odd particle orbit, but also some of the smaller details such as the peculiar influence of the Coriolis force on the  $M1$  transitions are similar.

#### 4.1.3. The $O(6)$ limit

For the general case of a particle coupled to a  $O(6)$  core, it is more difficult to construct approximate eigenstates and to construct an approximate expression for the excitation

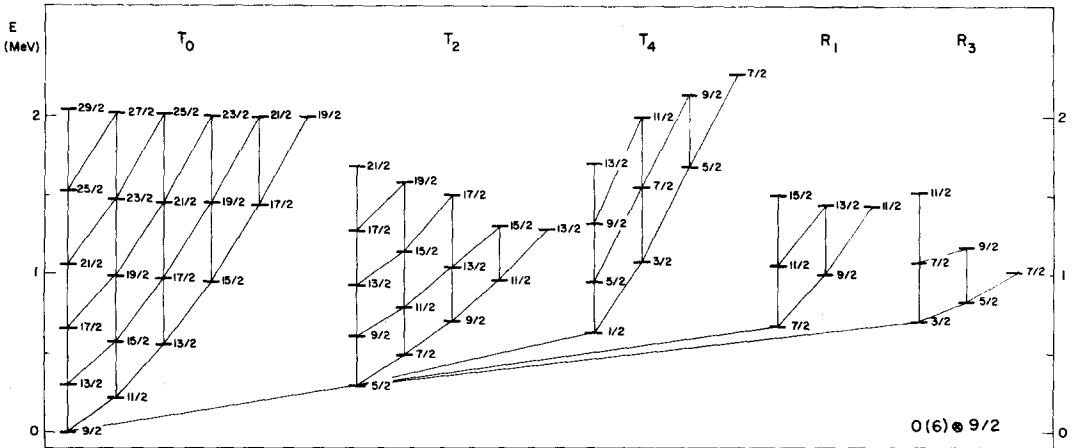


Fig. 9. A typical spectrum in the  $O(6)$  limit. A  $j = 9/2$  particle is coupled to an  $O(6)^{(4)}$  core ( $N = 6, A = 0.200$  MeV,  $B = 0.225$  MeV,  $C = 0$ ) with a pure  $O(6)$  quadrupole force given by  $v^2 = 0, \Gamma_0 = 0.023$  MeV,  $\Lambda_0 = 0$  and  $\chi = 0$  in eqn. (4.1.2). The lines connecting the levels denote large  $E2$  transitions.

energies. For certain specific values of  $j$  there exists, however, an exact solution that can be constructed by using a group theoretical approach. The occurrence of symmetries for odd mass nuclei will be discussed in Section 5.

A typical calculated spectrum is shown in Fig. 9. The groundstate is now no longer the bandhead of a well developed rotational band, but rather the lowest level of a complex multiplet labeled by  $T_0$  in the figure. The members of this multiplet are connected by strong  $E(2)$  transitions. At an excitation energy of only about 0.5 MeV one observes other multiplets with a similar structure as the  $T_0$  multiplet. The multiplets  $T_n$  are built on a level with  $k = j - n, n = \text{even}$ . The energy of the bandhead is roughly proportional to  $n$ . Within each multiplet the levels can be classified through the introduction of a quantum number  $\tilde{\tau} = 0, 1, 2, \dots$ , which is analogous to the seniority quantum number introduced in the  $O(6)$  dynamical symmetry. The angular momenta contained in each  $\tilde{\tau}$  multiplet is given by  $J = k + 2\tilde{\tau}, k + 2\tilde{\tau} - 1, \dots, k + \tilde{\tau}$ . As in the  $O(6)$  limit the  $E2$  transitions connect only levels with

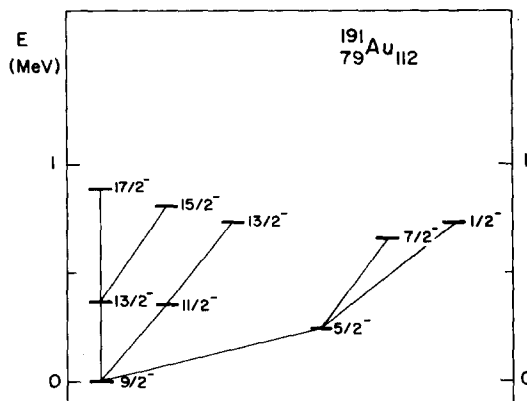


Fig. 10. The experimental spectrum<sup>(54)</sup> built on the  $h_{9/2}$  proton configuration in  $^{191}\text{Au}_{112}$ .

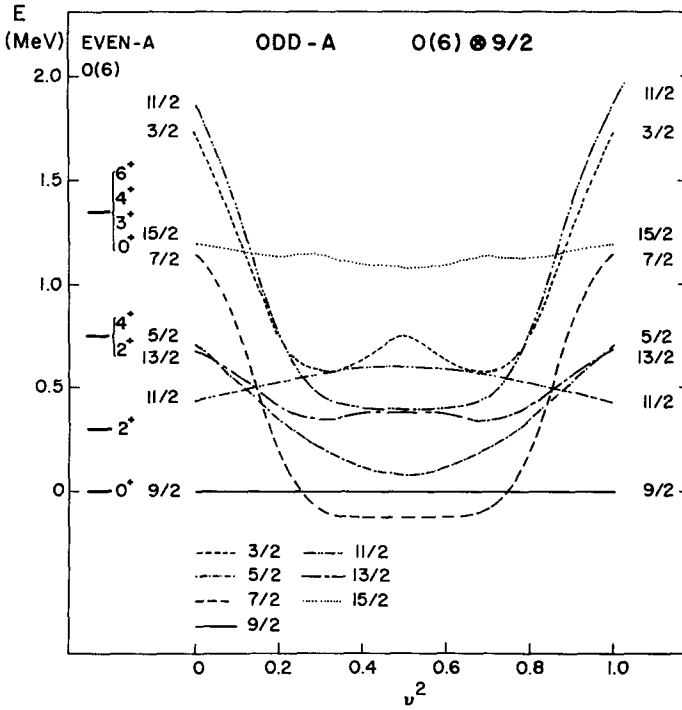


Fig. 11. Calculated low-lying levels for the system of a  $j = 9/2$  particle coupled to  $O(6)$  core<sup>(4)</sup> ( $N = 9$ ,  $A = 0.4$  MeV,  $B = 0.450$  MeV,  $C = 0$ ) as a function of  $v^2$  using eqns. (4.1) and (4.2) with  $\Gamma_0 = 0.567$  MeV,  $\Lambda_0 = 1.83$  MeV and  $\chi = 0$ .

$\Delta\tilde{\tau} = 1$ . As an example of the occurrence of spectra of this kind in nuclei, Fig. 10 shows the spectrum of <sup>191</sup>Au which is built on the  $h_{9/2}$  single-particle orbit.

In Fig. 11 the calculated levels as a function of the occupation probability  $v^2$  are shown. The figure is symmetric around  $v^2 = 0.5$  since, by taking the  $O(6)$  quadrupole operator with  $\chi = 0$ , the quadrupole force does not have any diagonal matrix elements in a weak coupling basis. With increasing  $v^2$  the energy of the  $J = j - 1$  level drops rapidly initially but stays approximately constant for  $0.3 < v^2 < 0.7$ . A similar behavior has also been observed in the  $\gamma$ -unstable rotor plus particle model of Wilets and Jean.<sup>(49,55)</sup>

#### 4.2. The Europium isotopes

The IBFA model can also be applied to transitional nuclei. Several different examples can be found in the literature,<sup>(56,57)</sup> but only the case of the odd-mass Europium isotopes will be discussed here. The Eu isotopes are considered since they contain examples of well deformed, spherical as well as transitional spectra. Only the properties that depend strongly on the s.p. structure of the levels will be mentioned here, a more complete account of the calculation is given in Ref. 57.

In the phenomenological calculations the Hamiltonian discussed in the previous section was used. To describe the Eu isotopes ( $Z = 63$ ) the odd proton is coupled to a Sm ( $Z = 62$ ) core with the same number of neutrons. The Sm isotopes have been discussed in terms of the IBA model in Ref. 32. On the basis of the single-particle energies it is to be expected that the

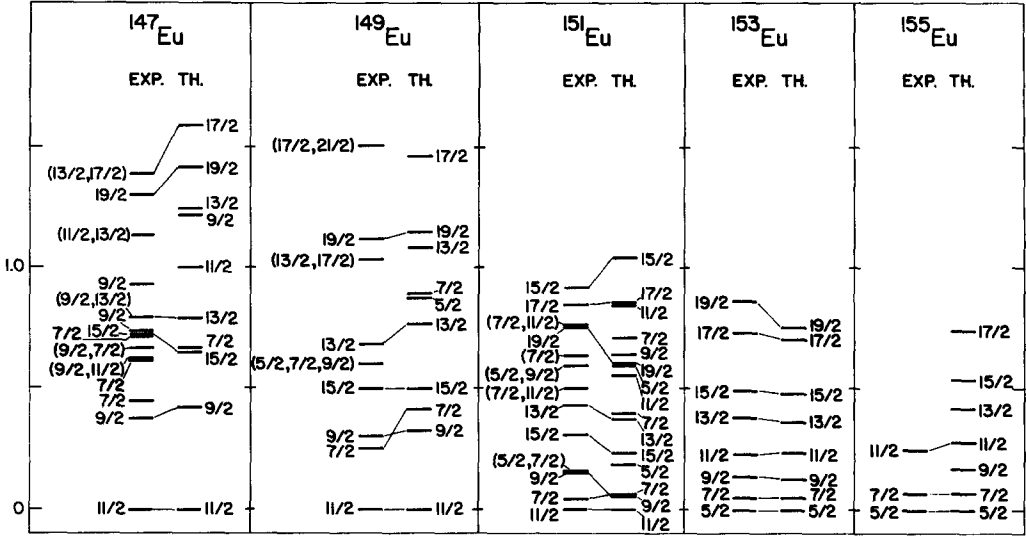


Fig. 12. Experimental<sup>(57-62)</sup> and calculated<sup>(56)</sup> excitation energies of negative parity states in the odd-mass Eu isotopes.

negative parity levels are based on the  $h_{11/2}$  s.p. orbit while the positive parity levels are based on the  $d_{5/2}$  and  $g_{7/2}$  orbits. To simplify the calculations it is assumed that the occupancies for the positive parity orbits are the same,  $v_+^2 = v_{5/2}^2 = v_{7/2}^2$ . By inspection of eqns. (3.22) and (3.23) it is clear that for this special case the interaction only depends on  $\gamma_\pi$  and  $\lambda_\pi$  defined as

$$\begin{aligned}\gamma_\pi &= (u_\pi^2 - v_\pi^2)\Gamma_{0x}, \\ \lambda_\pi &= u_\pi^2 v_\pi^2 \Lambda_{0x}; \quad \pi = +, -\end{aligned}\quad (4.11)$$

which implies that only two of the three parameters are independent.

The results of the calculation are compared with experiment in Fig. 12 for negative parity states and in Fig. 13 for positive parity. In the lighter isotopes, <sup>147,149</sup>Eu, the lowest states are the single-particle levels. At an energy  $\epsilon$ , the excitation energy of the  $2^+$  state in the core, one sees a multiplet of levels as expected in a weak-coupling scheme. In the heavier isotopes a completely different picture emerges. The lowest negative parity level is the band head of a  $K = 5/2^-$  rotational band. The fact that this band is the lowest depends in the phenomenological calculations on the ratio of the strengths of the exchange and the quadrupole forces. In a Nilsson scheme picture this implies that the fermi-surface is near  $K = 5/2$  and thus that the spherical  $h_{11/2}$  level is approximately 40% filled, i.e.  $v^2 \sim 0.3$  as has been taken in the IBFA calculations. For the positive parity levels the change across the transitional region may look less dramatic since the  $5/2$  state is the lowest level for all isotopes. A closer look shows that the changes in the spectrum are large indeed.

The level degeneracies observed in the positive parity spectra of <sup>151,153</sup>Eu can be explained in terms of a pseudo spin symmetry.<sup>(68)</sup> Such a symmetry occurs in the IBFA Hamiltonian whenever the two s.p. orbits with adjacent spins ( $j = 5/2$  and  $7/2$ ) that are coupled to the system of bosons have equal quasi-particle energies and equal occupation probabilities. In this case the angular momentum of the s.p. orbits can be decomposed into a pseudo orbital part coupled to a spin  $1/2$ ,  $j = \ell \pm 1/2$ . This pseudo orbital angular momen-



tum ( $\ell = 3$  in the present case) is in general not equal to the real s.p. value. Since the quadrupole operator acts only on the orbital angular momentum the calculated energies are independent of the orientation of the spin. All levels, with the exception of some  $J = 1/2$  levels, thus occur in doublets with  $J = L \pm 1/2$ . In  $^{151}\text{Eu}$  the groundstate is a member of a  $L = 3$  doublet while in  $^{153}\text{Eu}$  it has  $L = 2$ . This difference accounts for the fact that for

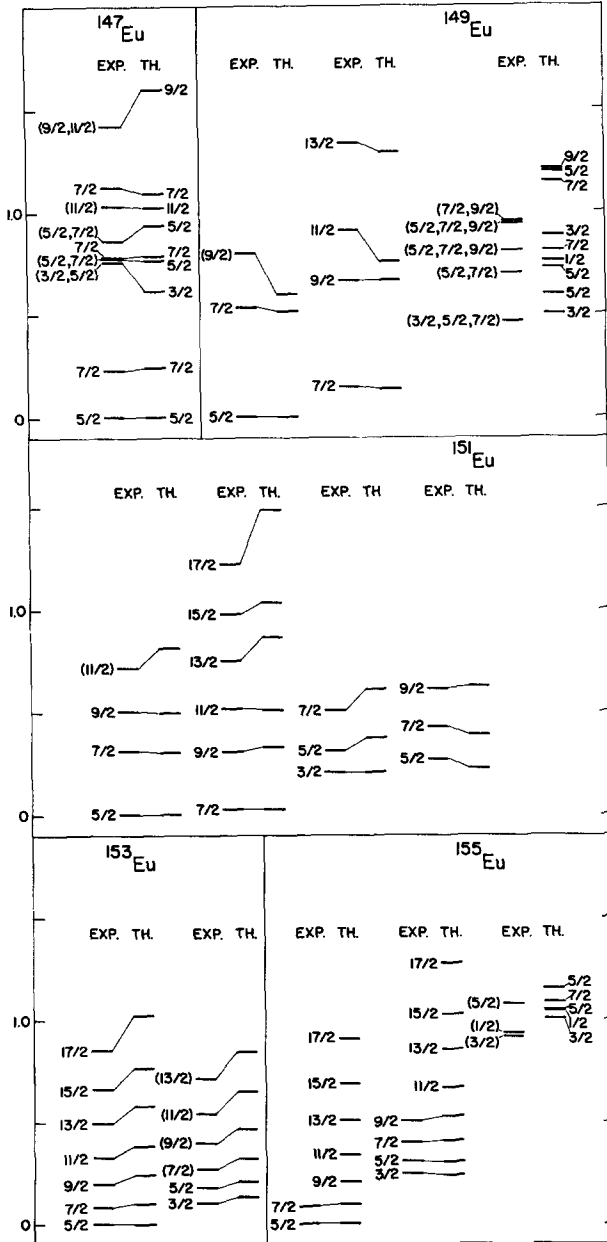


Fig. 13. Experimental<sup>(57-62)</sup> and calculated<sup>(56)</sup> excitation energies of positive parity states. For some levels the spin assignment is tentative.

<sup>151</sup>Eu there is an appreciable s.p. transfer spectroscopic factor to the groundstate while for <sup>153</sup>Eu it completely vanishes as will be discussed later.

Using the wave functions obtained from the energy calculations, transition probabilities can be calculated. The lowest order magnetic dipole operator can, in general, be written as a sum of two parts,

$$T^{(1)} = T_B^{(1)} + T_F^{(1)}, \quad (4.12)$$

where the first term acts only on the bosons

$$T_B^{(1)} = g_d(d^\dagger \tilde{d})^{(1)} \sqrt{\frac{30}{4\pi}}. \quad (4.13)$$

In the calculation of M1 properties for even-even nuclei higher-order terms in the operator have to be considered since in the IBA model space (4.13) is diagonal. In the calculation of magnetic moments which we will present here (4.13) gives a good enough approximation since they are predominantly determined by the fermion part of the operator,

$$T_F^{(1)} = - \sum_j g_{jj'} \sqrt{\frac{j(j+1)(2j+1)}{4\pi}} (a_j^\dagger \tilde{a}_{j'})^{(1)}, \quad (4.14)$$

where

$$g_{jj'} = \begin{cases} [(2j-1)g_\ell + g_s]/2j & j = j' = \ell + 1/2 \\ [(2j+3)g_\ell - g_s]/2(j+1) & j = j' = \ell - 1/2 \\ (g_\ell - g_s) \sqrt{\frac{2\ell(\ell+1)}{j(j+1)(2j+1)(2\ell+1)}} & j' = j-1; \ell = \ell' \end{cases}$$

where  $\ell$  is the s.p. orbital angular momentum. The  $d$ -boson  $g$ -factor can be extracted from the  $g$ -factor of the  $2_1^+$  in the Sm isotopes,  $g_d = 0.32$  n.m. Using the s.p. value for  $g_\ell = 1.0$  n.m. and  $g_s = 5.5885$  n.m. the magnetic moments are over estimated by about 20%. In the calculation shown in Fig. 14,  $g_s = 4.0$  n.m. was used, representing a quenching of about a factor 0.7. This quenching is similar to what has been used in recent calculations for the  $N = 82$  isotones in the shell-model.<sup>(69)</sup>

The image of the shell model single nucleon creation operator  $c_j^\dagger$  [eqn. (3.10)] should, in principle, be used in the calculation of s.p. transfer amplitudes. The fact, however, that (2.7) is only a lowest order estimate to the full operator gives rise to the fact that sum-rules such as  $c_j^\dagger c_j + c_j c_j^\dagger = 1$  are no longer obeyed. In order to restore these, normalization factors  $K_j^a$  and  $K_j^b$  have been introduced.

$$A_j^\dagger = \left[ u_j a_j^\dagger - \sum_{j'} \frac{v_j}{\sqrt{N_\pi}} \sqrt{\frac{10}{2j+1}} \frac{N_\pi}{N} \beta_{j'j}(\mathbf{K}_\beta)^{-1} s^\dagger (\tilde{d} a_{j'})^{(j)} \right] / K_j^a \quad (4.15)$$

describes the stripping of a fermion without changing the number of bosons in the core and

$$B_j^\dagger = \left[ \frac{v_j}{\sqrt{N}} (s^\dagger \tilde{a}_j)^{(j)} + \sum_{j'} u_j \sqrt{\frac{10}{2j+1}} \sqrt{\frac{N_\pi}{N}} \beta_{j'j}(\mathbf{K}_\beta)^{-1} (d^\dagger \tilde{a}_{j'})^{(j)} \right] / K_j^b \quad (4.16)$$

describes the stripping of a fermion on an odd nucleus with  $N$  bosons leading to a  $(N+1)$  boson even mass nucleus. The normalization factors are determined by

$$\sum_{\text{odd}} \langle \text{odd} | A_j^\dagger | \text{even} \rangle^2 = (2j+1)u_j^2$$

and

$$\sum_{\text{odd}} \langle \text{even} | B_j^\dagger | \text{odd} \rangle^2 = (2j+1)v_j^2. \quad (4.17)$$

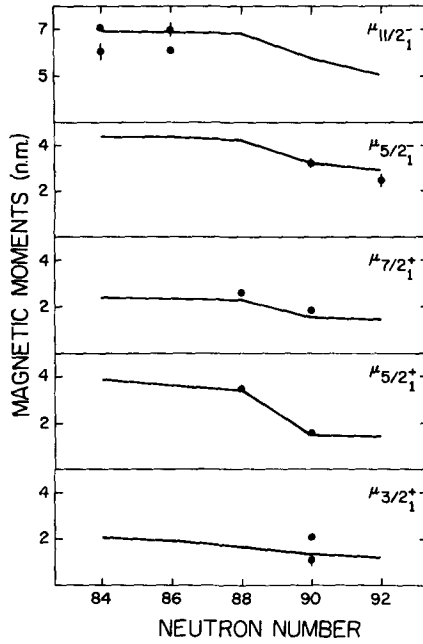


Fig. 14. Experimental<sup>(63,64)</sup> and calculated<sup>(56)</sup> magnetic moments for some levels in the Eu isotopes.

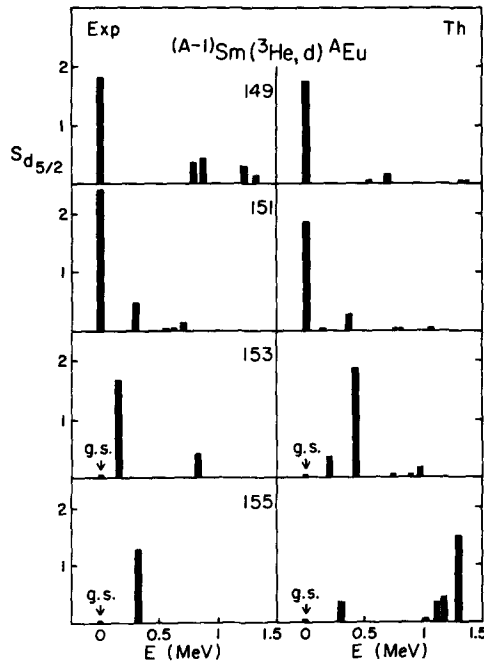


Fig. 15. The experimental<sup>(57,66,67)</sup> and calculated<sup>(56)</sup> spectroscopic factors for  $d_{5/2}$  transfer in  $A-1\text{Sm}(^3\text{He}, d)^A\text{Eu}$  as a function of excitation energy. Note that the  $5/2_1^+$  level lies at zero excitation energy for all isotopes. Only the strength definitely assigned to  $d_{5/2}$  transfer has been plotted.

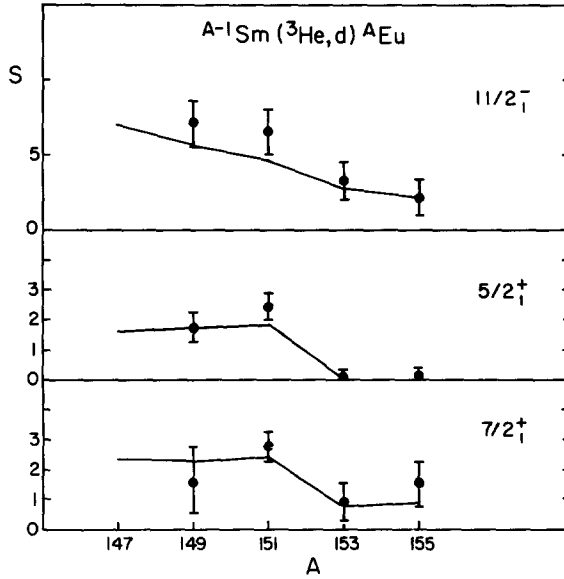


Fig. 16. Spectroscopic factors<sup>(57,66,67)</sup> for  $h_{11/2}$ ,  $d_{5/2}$  and  $g_{7/2}$  transfer for the first level of each spin.

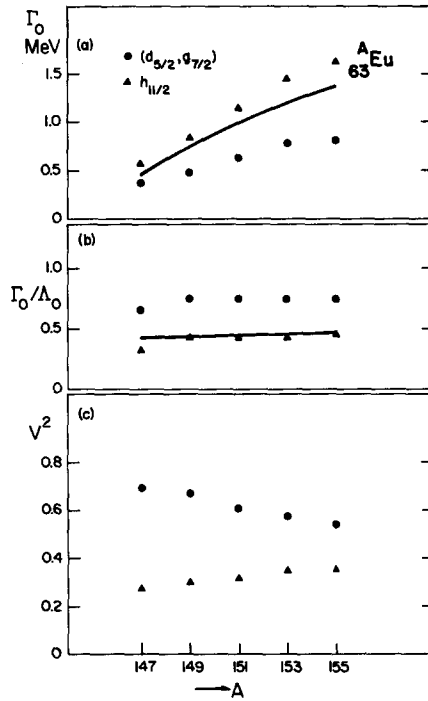


Fig. 17. Deduced values for the parameters  $\Gamma_0$ ,  $\Lambda_0$  and  $v^2$  as discussed in the text. The curves give the microscopic estimates as obtained from eqns. (3.24) and (3.25).

Calculated spectroscopic factors are compared with experiment in Figs 15 and 16. The calculation does not have any adjustable parameters.

The spectroscopic factors for even to odd for the first levels of each spin show, in general, a steady decrease toward the more deformed nuclei. This can easily be explained by the fact that the coupling is much stronger for deformed nuclei. A striking feature is that for  $^{153}\text{Eu}$  and  $^{155}\text{Eu}$  the spectroscopic factor for the  $5/2_1^+$  level is vanishingly small. As was discussed above, in  $^{151}\text{Eu}$  the  $5/2_1^+$  and the  $7/2_1^+$  levels belong to an  $L = 3$  doublet in the pseudo spin picture<sup>(68)</sup> and can be excited in s.p. transfer. The same holds for the  $5/2_2^+$  and  $7/2_2^+$  levels in  $^{153}\text{Eu}$  and  $^{155}\text{Eu}$ . In  $^{153}\text{Eu}$  and  $^{155}\text{Eu}$  the  $5/2_1^+$  level belongs, however, together with the  $3/2_1^+$  level, to a  $L = 2$  doublet which has a zero excitation probability since the pseudo orbital angular momentum of the coupled s.p. levels is  $\ell = 3$ .

In order to extract values for  $\Lambda_{0\pi}$  and  $\Gamma_{0\pi}$  from the fitted parameters  $\gamma_\pi$  and  $\lambda_\pi$ , some additional conditions have to be imposed. One of the extra conditions is obviously that  $\Sigma_j v_j^2(2j+1) \simeq n$ , the number of valence nucleons. The other condition is that the ratio  $\Gamma_{0\pi}^2/\Lambda_{0\pi} = R_\pi$  is the same for positive and negative parity. This last condition has been imposed since the radial integrals, which are not equal for positive and negative parity orbits, appear quadratically in  $\Lambda_0$  and only linearly in  $\Gamma_0$ . The extracted values for  $\Lambda_0$  and  $\Gamma_0$  are plotted in Fig. 17 where they are compared with the results of a microscopic calculation, eqns. (3.24) and (3.25) with  $\bar{\kappa} = 2 \text{ MeV}$  for positive parity and  $\bar{\kappa} = 3.4 \text{ MeV}$  for the negative parity parameters. This large difference between the two extracted values for  $\bar{\kappa}$  is still an open problem. It can partly be attributed to a stronger neutron-proton interaction for the  $h_{11/2}$  orbit since this proton orbit belongs to a harmonic oscillator shell with the same quantum numbers as the valence neutrons. Using eqn. (3.26) a strength for the boson-boson quadrupole interaction can be determined,  $\kappa = -1.1 \text{ MeV}$  which is much larger than the typical values used in the phenomenological calculations,<sup>(6)</sup>  $\kappa = 0.1-0.3 \text{ MeV}$ . This discrepancy might be explained in part in terms of an effective interaction since in the IBFA model calculations the basis space for the odd particle is very much truncated. Part of the difference might also be the result of the interaction between like particles which has not been considered in the microscopic derivation.

### 4.3. Spreading width of deeply bound hole states

A last application of the model involves the calculation of the spreading width of deeply bound hole states.<sup>(70)</sup> Single particle pick-up reactions can occur on nucleons in the valence shell. This, in general, will lead to the low-lying states in the final nucleus. The reaction can also occur on nucleons in core orbits which will lead to highly excited states, typically at an excitation energy of around 5 to 10 MeV. At this energy the level density is of such a magnitude that individual states can no longer be resolved experimentally. In spite of this one can determine the single particle transfer strength distribution as a function of excitation energy. As can be seen in Fig. 18 there is a considerable amount of structure in the strength distribution.<sup>(70)</sup>

The strength distribution can be calculated in a kind of doorway model in which the single-particle couples most strongly to the low-lying collective states. Since the density of collective states is rather small, this coupling will distribute the strength over a few discrete states. These collective states couple to the background of non collective states which will give rise to an additional spreading.

The coupling of the deeply bound hole state to the low-lying collective states can be described in the IBFA model. Since the orbit under consideration is completely filled

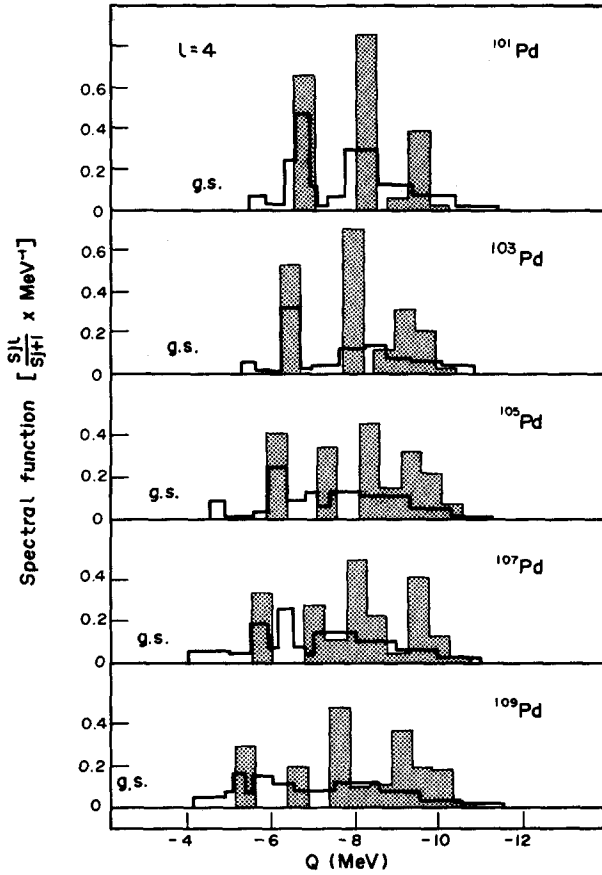


Fig. 18. Distribution functions of spectroscopic strength for the  $g_{9/2}$  orbit as obtained in the  $^{A+1}\text{Pd}(d,t)^A\text{Pd}$  reaction<sup>(70)</sup> are compared with the results of the IBFA calculation. The calculated strength has been binned in 0.5 MeV intervals.

( $v^2 = 1$ ) the exchange force vanishes and the fermion couples to the bosons only via the quadrupole term. Also the single-particle transfer operator simplifies considerably since the second term in eqn. (4.0) vanishes. In Fig. 18 the calculated spectroscopic factors are given. In the Hamiltonian the parameters have been adjusted to give a best overall agreement  $\Gamma_0 = 2.25$  MeV,  $A_0 = -0.126$  MeV independent of mass number. The calculation correctly reproduces the structure of the observed  $g_{9/2}$  strength distribution in  $^{101}\text{Pd}$  and furthermore the fact that with increasing mass the spreading of the strength increases dramatically.

## 5. BOSON-FERMION SYMMETRIES

A different approach to odd-mass nuclei, more phenomenological in nature, is based upon the use of dynamical symmetries. In spirit this is very similar to the introduction of dynamical symmetries to describe the spectra of even-mass nuclei in the IBA model.<sup>(2,3,4)</sup> In the application to odd-mass nuclei a complication arises from the fact that one has to deal simultaneously with both bosonic and fermionic operators. This is treated by the intro-

duction of supersymmetries. These supersymmetries offer a rich group structure<sup>(71)</sup> which to date has only been partly explored. In the following, therefore, only a short outline of the concept is given.

As is well known one can discuss the IBA-1 model for even-even nuclei in terms of symmetry groups.<sup>(2,3,4)</sup> The symmetry group related to the IBA-1 model is  $G = U(6)$ . The six dimensions are formed by the five components of the  $d$ -boson combined with the single component of the  $s$ -boson. The group is the unitary group since it leaves the norms (total number of bosons) invariant. Using the methods of group theory three chains of subgroups of the  $U(6)$  group can be constructed. If the Hamiltonian can be expressed in terms of Casimir invariants of one of these chains only, the energy spectrum can be obtained analytically. The spectra appear to be characteristic of three different physical geometries, the  $U(5)$  chain<sup>(2)</sup> gives a vibrational spectrum, the  $U(3)$  chain<sup>(3)</sup> that of an axially symmetric rotor while the  $O(6)$  chain<sup>(4)</sup> gives rise to a spectrum typical of a  $\gamma$  unstable rotor.

For the case of a fermion coupled to the system of bosons a group structure also exists and one can construct chains of subgroups and calculate the energy spectrum in closed form. These Bose Fermi symmetries can be constructed only for certain values of the spin of the odd particle. Several examples of super symmetries have been discussed in the literature.<sup>(71-80)</sup> Only the case of a  $j = 3/2$  particle coupled to an  $O(6)$  core will be treated here. A  $j = 3/2$  particle forms a representation of the  $U(4)$  group since it has four different  $m$ -states. The  $U(4)$  group is isomorphic with the  $O(6)$  group and the product of the two groups contains a subgroup, referred to as  $\text{Spin}(6)$ , with a Lie algebra similar to that of the  $O(6)$  and  $U(4)$  groups. Physically, the fact that the product  $O^B(6) \otimes U^F(4)$  contains  $\text{Spin}(6)$  as a subgroup, implies that the parameters describing the boson system are in a unique relation to the parameters describing the boson-fermion and the fermion interaction. The fact that symmetries are observed in the spectra of odd-mass nuclei shows that apparently this relation is satisfied in nature. The chain of subgroups can be written as

$$U^B(6) \otimes U^F(4) \supset O^B(6) \otimes U^F(4) \supset \text{Spin}(6) \supset \text{Spin}(5) \supset \text{Spin}(3) \supset \text{Spin}(2) \quad (5.1)$$

where the superscripts  $B$  or  $F$  indicate that the group contains boson or fermion operators. If the Hamiltonian is expressed as a sum of Casimir operators for the different sub-groups the eigenstates can be labeled by the quantum numbers labeling the different representations of the groups. The quantum numbers of the different subgroups are  $[N]$  for  $U^B(6)$ ,  $\{M\}$  for  $U^F(4)$ ,  $\Sigma$  for  $O^B(6)$ ,  $(\sigma_1, \sigma_2, \sigma_3)$  for  $\text{Spin}(6)$ ,  $(\tau_1, \tau_2)$  for  $\text{Spin}(5)$ ,  $J$  for  $\text{Spin}(3)$  and  $M_J$  for  $\text{Spin}(2)$ . The expression for excitation energies can now be written as

$$E_x = -\frac{A}{4} [\sigma_1(\sigma_1 + 4) + \sigma_2(\sigma_2 + 2) + \sigma_3^2] + \frac{B}{6} [\tau_1(\tau_1 + 3) + \tau_2(\tau_2 + 1)] + CJ(J + 1) + D\Sigma(\Sigma + 4) \quad (5.2)$$

The coefficients  $A, B, C, D$  multiply the Casimir operators in the Hamiltonian. It is seen that this simple formula can describe the excitation energies observed in  $^{192}\text{Pt}$  and  $^{191}\text{Ir}$  (Figs 19, 20) quite well. Also, electromagnetic and single-particle transition rates and selection rules calculated in the symmetry scheme agree<sup>(78-80)</sup> with the experimental observations. Boson fermion symmetries are thus very useful to introduce an ordering for the levels in the otherwise very complicated spectrum of an odd-mass nucleus.

We note that the spectra of both the odd- and even-mass nuclei (Fig. 19), can be described by eqn. (5.2) with the same set of parameters. This indicates the validity of a super symmetry scheme in which the even- and odd-mass nuclei are described simultaneously in terms of the

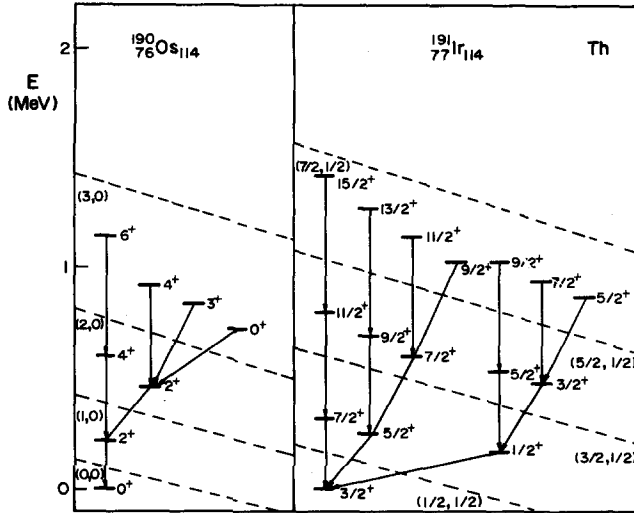


Fig. 19. Calculated<sup>(79)</sup> spectra using eqn. (5.2) with  $B/6 = 40$  keV and  $C = 14$  keV. The numbers in parenthesis denote the Spin(5) labels  $(\tau_1, \tau_2)$ .

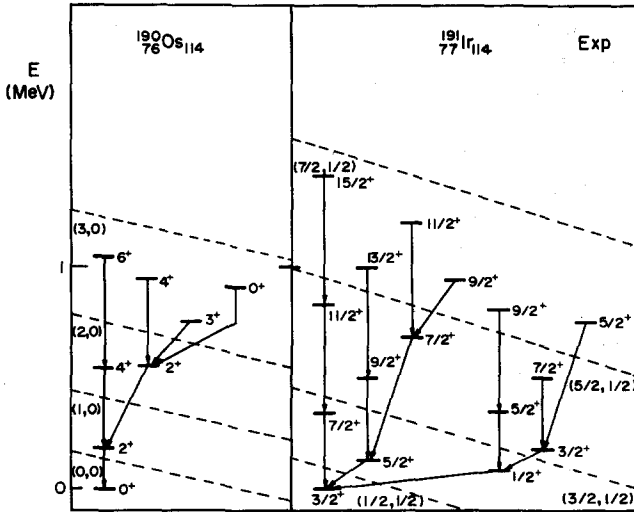


Fig. 20. Experimental<sup>(81,82)</sup> spectra for  $^{190}\text{Os}$  and  $^{191}\text{Ir}$ .

subgroups of a single super symmetry group. For the case discussed here the supergroup<sup>(78-80)</sup> is  $U(6/4)$  which contains  $U^B(6) \times U^F(4)$  as a subgroup.

Other groups that are of much current interest are<sup>(77)</sup>  $U(6/2)$  and<sup>(71-76)</sup>  $U(6/12)$ . The latter describes the case in which  $j = 1/2, 3/2$  and  $5/2$  orbits are coupled to the system of bosons. This group, like  $U(6/4)$  contains an  $O(6)$  subgroup which can be reached in two different group reductions.

$$I. \quad U(6/12) \supset U^B(6) \otimes U^F(6) \otimes U^F(2) \supset SO^B(6) \otimes SO^F(6) \otimes U^F(2) \supset SO^{BF}(6) \otimes U^F(2)$$



or

$$\text{II. } U(6/12) \supset U^B(6) \otimes U^F(6) \otimes U^F(2) \supset U^{BF}(6) \otimes U^F(2) \supset SO^{BF}(6) \otimes U^F(2) \dots$$

The group reduction chain I is discussed in Ref. 71 while II is discussed in Refs 72 and 73. The two group reduction schemes allow for a different form of the Hamiltonian and give rise to different expressions for the excitation energies which are given in the original references. Applications of the two dynamical symmetries to the spectrum of  $^{195}\text{Pt}$  indicate that chain II allows for a better agreement with the data. By introducing terms in the Hamiltonian that are quadratic in the Casimir operators the dynamical symmetry remains unbroken but a significantly better agreement<sup>(74)</sup> can be obtained with the data. Introduction of terms in the Hamiltonian that are quadratic in the Casimir operators imply the presence of three-body terms in the Hamiltonian. In a microscopic derivation of the boson-fermion interaction one indeed obtains terms of this order as a result of the action of the Pauli principle between the bosons and the odd fermion. In the interaction used in the IBFA model, however, only terms second order in the boson operators are retained.

## 6. TWO QUASI-PARTICLE DEGREES OF FREEDOM

The approach that has been presented in the previous sections for coupling one quasi-particle (q.p.) degree of freedom can be extended to include the description of two quasi-particle degrees of freedom in the nucleus. In the cases in which these modes exhibit a certain degree of collectivity they can be treated as a collective mode, different from the  $s$ - and  $d$ -bosons. Examples of these collective 2 q.p. modes are the  $g$ -boson<sup>(83-86)</sup> and the  $f$ -boson<sup>(9)</sup> that have been coupled to the IBA bosons to explain low-lying  $K = 3^+$  bands in deformed nuclei and low-lying negative parity states. Another example is formed by the low-lying  $0^+$  state in the Ge and Se isotopes. This state is also based upon a collective  $L = 0, 2$  q.p. excitation. Since this collective  $L = 0$  degree of freedom is different from the  $s$ -boson in the IBA model, it is denoted by  $s'$ . The giant dipole resonance is an example of a high-lying collective 2 q.p. excitation and has been calculated in the IBA model by coupling a  $P$ -boson with an energy of about 15 MeV to the system of  $s$ - and  $d$ -bosons.<sup>(87-89)</sup> In some cases as, for example, in explaining back bending phenomena this procedure of bosonization of the 2 q.p. mode cannot be applied and the 2 q.p. states have to be treated explicitly.<sup>(90-92)</sup> In Ref. 92 these two quasi-particle degrees of freedom have been treated in a phenomenological approach. In Ref. 91 however the 2 q.p. states are described on the basis of a semimicroscopic theory, similar to that which was used to describe odd-mass nuclei in the IBFA model.

### 6.1. Microscopic treatment

The outline of the microscopic treatment of two quasi-particle states in the IBA model given here closely follows the approach taken by Morrison *et al.* in Ref. 91 to which reference should be made for the finer details.

The microscopic basis for the coupling of the 2 q.p. model is discussed most readily in a basis where neutron and proton degrees of freedom are treated explicitly. The approach followed is very similar to that used in deriving the boson-fermion interaction for the IBFA model, discussed in Section 3. The main difference is that while in the IBFA model only basis states with a single odd-particle are considered, here a mixture of pure  $N$  - boson states and states with  $(N - 1)$  bosons coupled to two quasi-particles is considered. In principle these

states are not completely orthogonal, but the overlap vanishes in the limit of a very collective boson. Assuming that the neutrons are well described in terms of a system of bosons and that two quasi-particle excitations only have to be considered explicitly for the protons, the Hamiltonian for the full system can be written as

$$H = H_B + H_{F\pi} + V_{\pi\pi} \quad (6.1)$$

where  $H_B$  is the boson Hamiltonian describing the neutron excitations. The part of the Hamiltonian describing the protons can be written in general, without the introduction of collective degrees of freedom as

$$H_F = \sum_{jm} \varepsilon_j c_{jm}^\dagger c_{jm} + \sum'_{JM} V_{abcd}^J A_{ab}^\dagger(JM) A_{cd}(JM). \quad (6.2)$$

In the following, this part of the full Hamiltonian will be considered more closely and boson and 2 q.p. degrees of freedom will be introduced simultaneously. In eqn. (6.2) and the following equations the prime indicates that the summation over single particle orbits should be restricted to  $a \leq b$  and  $c \leq d$ . The two particle creation operator is defined according to

$$A_{ab}^\dagger(JM) = (1 + \delta_{ab})^{-1/2} [c_a^\dagger c_b^\dagger]_M^{(J)}. \quad (6.3)$$

The operators  $c_j^\dagger$  are the real shell model single nucleon creation operators. As in Section 2 the neutron-proton interaction is taken to be a pure quadrupole interaction,

$$V_{\pi\pi} = \kappa_{\pi\pi} Q_B^{(2)} \cdot q_F^{(2)}$$

where  $q_F$  and  $Q_B$  are defined in eqns. (2.5) and (2.7).

The interaction between like particles can be rewritten in terms of boson and odd nucleon operators by replacing the shell model operators  $c_j^\dagger$  and  $c_j$  by their image  $\check{c}_j^\dagger$  and  $\check{c}_j$  in the boson fermion space as given in eqn. (3.10). The Hamiltonian can now be contracted into three parts; (a) one that contains only boson operators. This part gives rise to the usual IBA Hamiltonian as is discussed in Section 2; (b) A part that contains only odd particle operators. This part can be written as<sup>(91)</sup>

$$H_2 = \sum_{j,m} \tilde{\varepsilon}_j a_{jm}^\dagger a_{jm} + \sum'_{JM} (u_a u_b u_c u_d + v_a v_b v_c v_d) V_{abcd}^J A_{ab}^\dagger(JM) A'_{cd}(JM) + \sum'_{JM} u_a v_b u_c v_d \bar{V}_{abcd}^J A'_{ad}^\dagger(JM) A'_{bc}(JM) \quad (6.4)$$

where the two quasi-particle operator is defined in terms of the odd particle operators as

$$A'_{ab}^\dagger(JM) = (1 + \delta_{ab})^{-1/2} [a_a^\dagger a_b^\dagger]_M^{(J)}. \quad (6.5)$$

The particle hole interaction strength is given by

$$\bar{V}_{adbc}^J = 4 \sum'_J V_{abcd}^J (-1)^{b+c+J} (2J'+1) \left\{ \begin{matrix} a & b & J' \\ c & d & J \end{matrix} \right\} \left[ \frac{(1 + \delta_{ad})(1 + \delta_{bc})}{(1 + \delta_{ab})(1 + \delta_{cd})} \right]^{1/2} \quad (6.6)$$

in terms of the particle-particle interaction. The third part (c) contains terms that change the number of bosons. For  $J = 0$  in eqn. (6.2) these terms correspond to the  $H_{02} + H_{20}$  two quasi-particle changing terms in BCS. In a generalized seniority scheme these terms correspond to  $\Delta w = 2$  terms in the Hamiltonian. The  $s$  bosons can be defined such that these terms vanish exactly.<sup>(21)</sup> A similar approach is taken in the BCS theory. For  $J = 2$  this is not

possible and a term

$$H_{BF}^2 = \sqrt{2} \sum'_{abcd} V_{abcd}^2 (-1)^{c-d} (u_a u_b u_c u_d + v_a v_b v_c v_d) \beta_{dc} (1 + \delta_{cd})^{-1/2} (A_{ab}^\dagger(2) \cdot \vec{d} + \text{h.c.}) \quad (6.7)$$

has to be included in the interaction. The coefficient  $\beta$  is defined in eqn. (2.3). Even though this interaction does not conserve the number of bosons, it does conserve the total number of particles which is one of the basic fundamentals of the IBA model. The boson operator appearing in eqn. (6.7) is, of course, of the same kind as the 2 q.p. operator, proton-like in the present example.

The neutron-proton interaction can be treated in a similar manner. As in the case of the like particle interaction it has three distinct parts, a boson-boson interaction which is the same as in the IBA model, a boson-fermion interaction that conserves the number of bosons and is the same as the IBFA interaction and a boson non-conserving interaction. This latter interaction can be simplified when projected<sup>(32)</sup> on the maximal  $F$  spin sub-space. Retaining only the terms of lowest (first) order in the boson operators this interaction can be written as<sup>(91)</sup>

$$H_{BF}^2 = \sum_j q_j^0 \{s^\dagger \cdot A_j'(0) + \text{h.c.}\} + \sum_{jj'} q_{jj'}^2 \{\vec{d} \cdot A_{jj'}^\dagger(2) + \text{h.c.}\} \quad (6.8)$$

where

$$q_j^0 = +2\sqrt{5}K_{\nu\pi} \sum_j (u_j u_j - v_j v_j) \beta_{jj'} (-1)^{j-j'} \frac{1}{j} q_{jj'} \sqrt{\frac{N_\pi}{N}} \quad (6.9)$$

and

$$q_{jj'}^2 = (1 + \delta_{jj'})^{-1/2} K_{\nu\pi} \beta_{jj'} \frac{N_\pi}{\sqrt{N}} \quad (6.10)$$

the total Hamiltonian for the coupled system can now be written as

$$H_{2qp} = H_{IBA} + V_{BF} + H_2 + H_{BF}^1 + H_{BF}^2 \quad (6.11)$$

where  $H_{IBA}$  is the usual IBA model Hamiltonian and  $V_{BF}$  the boson conserving interaction used in the IBFA model. The two body quasi-particle interaction  $H_2$  is defined by eqn. (6.4). The boson and two q.p. degrees of freedom are admixed as a result of the quadrupole pairing interaction between like particles,  $H_{BF}^1$  and as a result of the neutron-proton quadrupole force,  $H_{BF}^2$ .

## 6.2. Some applications

Two quasi-particle modes in even-even nuclei have been calculated in the above microscopic approach<sup>(91)</sup> and in some more phenomenological approaches.<sup>(83-86,93)</sup> Some examples of both will be given here.

### 6.2.1. Low spin states

The first type of intruder states that have been considered in the IBA model is a collective  $3^-$  state, an  $f$ -boson,<sup>(9)</sup> in order to be able to calculate negative parity states. Some of the first calculations of two quasi-particle states in the IBA model to explain low-lying positive parity intruder states are reported in Refs 83-86 and 93. In these calculations a more phenomenological approach has been taken.

In many medium-heavy and heavy nuclei relatively low-lying  $0^+$  states can be found

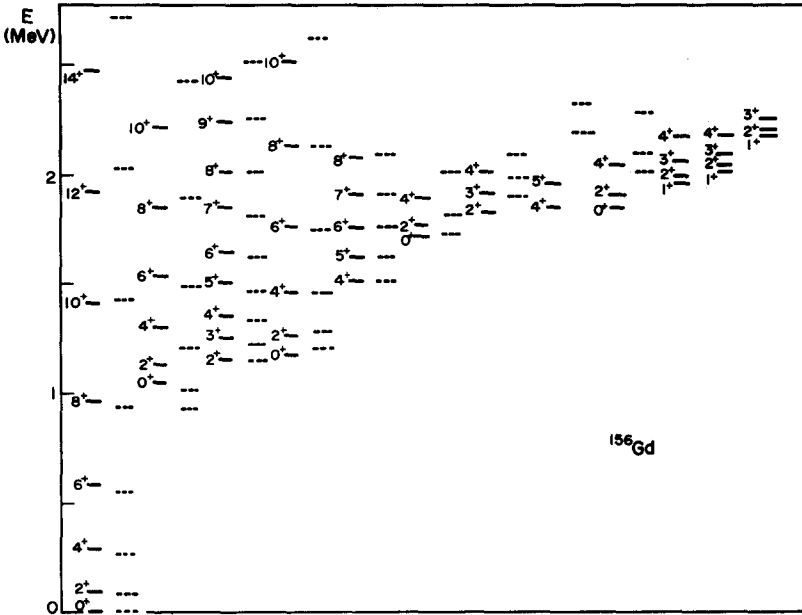


Fig. 21. Experimental<sup>(94)</sup> (drawn) and calculated<sup>(86)</sup> (dashed) spectrum of  $^{156}\text{Gd}$ .

which are not explained in the normal IBA model. Examples of this are  $0^+$  and  $2^+$  states around 1.4 MeV in  $^{112,114}_{48}\text{Cd}$  (Ref. 85); an additional  $K = 0^+$  rotational band in  $^{156}\text{Gd}$  (Refs 84, 86) and a  $K = 0^+$  band at  $E_x \simeq 0.5$  MeV in  $^{184,186}_{80}\text{Hg}$  (Ref. 93). The fact that all these nuclei are in the vicinity of a (sub)shell closure, ( $Z = 50$  for Cd,  $Z = 64$  for Gd and  $Z = 82$  for Hg) suggest that these intruder states have a strong 2p-2h nature. Since we are dealing here with some very low-lying states it can be assumed that the two particle excitation across the (sub)shell closure is collective. In the approaches taken in Refs 83–86 and 93 this mode is therefore taken into account as an excitation mode similar to that of the  $s$  boson, to distinguish the two it is denoted by  $s'$ . In Refs 85 and 93 this mode has been treated explicitly in the neutron proton formalism. In the present discussion I will limit myself to the work of Ref. 86.

The two quasi-particle states do not have to be limited to only  $s'$  modes but the formalism can easily be extended to include  $J = 2$  ( $d'$ ) and  $J = 4$  ( $g$ ) modes. The phenomenological Hamiltonian for this coupled system can be written as

$$\begin{aligned}
 H = H_{sd} + \varepsilon_{s'} n_{s'} + \varepsilon_{d'} n_{d'} + \varepsilon_g n_g - \kappa' Q^{(2)} \cdot Q^{(2)} - \kappa_g [Q^{(2)}(g^\dagger g)^{(2)}]^{(0)} \\
 + \xi' [(d^\dagger d^\dagger)^{(0)} s s' + \text{h.c.}]^{(0)} - \xi_g [(d^\dagger d^\dagger)^{(2)} (\bar{d} \bar{g})^{(2)} + \text{h.c.}]^{(0)} \quad (6.12)
 \end{aligned}$$

where  $Q^{(2)}$  is the quadrupole operator for the primed bosons. This Hamiltonian is used in Ref. 86 to calculate the spectrum of  $^{156}\text{Gd}$ , the results of which are displayed in Fig. 21. In this calculation the second excited  $0^+$  state is predominantly built on excitations involving the primed bosons. The low-lying  $K = 4^+$  band is built on a  $g$ -boson excitation. In Ref. 86  $B(E2)$  transitions are also calculated and found to agree with the available experimental data.

### 6.2.2. High spin states

Back bending phenomena observed for high spin states can be explained by the crossing

of the groundstate band and a two quasi-particle band. Because both the Coriolis anti-pairing effect and the rotation alignment effect increase with increasing angular momentum, the unique parity intruder orbitals such as  $h_{11/2}$  and  $i_{13/2}$  are most important in a description of this crossing. These two quasi-particle modes have been used to explain back bending phenomena in Kr in Ref. 90, in the Ba and Ce isotopes in Ref. 92 and in the Hg isotopes in Ref. 91. In most cases a satisfactory agreement between calculation and experiment is obtained. In the following, the application to the Hg isotopes is discussed in some more detail.

Recent  $g$  factor measurements<sup>(95)</sup> strongly suggest that in the Hg isotopes the  $i_{13/2}$  neutron orbit is the origin for the observed back bending and not the possibly competing<sup>(96)</sup>  $(h_{11/2})^2$  proton configuration. In the calculations presented in Ref. 91 therefore only configurations with up to 2 neutron quasi-particles in the  $i_{13/2}$  are considered. The coupling of the two-q.p. states to the boson is described by the Hamiltonian (6.11). The occupancies of the valence orbits  $v_j$  which enter in the definition of the parameters of the Hamiltonian [see eqns. (6.9) for example] were obtained from a Nilsson + BCS calculation.<sup>(97)</sup> In the  $O(6)$  limit<sup>(4)</sup> which is appropriate for these nuclei, the core Hamiltonian [ $H_{\text{IBA}}$  in eqn. (6.11)] can be described by<sup>(4)</sup>  $A = 0.47$  MeV,  $B = 0.6$  MeV and  $C = 0$ . The strength of the particle core interaction was obtained from a best fit to the levels based on the  $i_{13/2}$  s.p. state in the odd Hg isotopes,<sup>(91)</sup>  $\kappa = 0.05$  MeV and  $\kappa\chi = -0.083$  MeV. The interaction that enters in the definition of  $H_2$  [eqn. (6.4)] was taken to be a surface delta interaction with strength  $A_1 = 0.15$  MeV. In a calculation in which the  $0_2^+$  state in the core and the band built on top of it was omitted (the calculation without P.V. in Fig. 22) the strength of the interaction was increased to  $A = 0.18$  MeV, in rough agreement with the BCS pairing strength<sup>(97)</sup>  $G_n = 37/A$ . The calculated lowest levels of each spin in  $^{198}\text{Hg}$  are compared with experiment in Fig. 22. Overall agreement is good, both below and above the band crossing at  $J = 8^+$ . It should be noted that in the calculation even the low lying  $0_2^+$  level contains an admixture of two quasi-particle components of about 50%. This re-emphasizes the importance of including two q.p. degrees of freedom for nuclei near shell closures. In Ref. 91 calculations for excitation energies in  $^{194}\text{Hg}$  and  $^{196}\text{Hg}$ ,  $g$ -factors and  $B(E2)$  transitions are also compared with experiment. In general a good agreement is obtained.

### 6.3. Giant resonances

The spreading-width of Giant Resonances, specifically the Giant Dipole Resonance (GDR), has also been calculated using the IBA model.<sup>(87-89)</sup> Since states of this kind occur at the relatively high excitation energy of about 15 MeV, no discrete sharp states can be resolved any more due to the high level density. The situation is thus completely analogous to that of deeply bound hole states in odd-mass nuclei<sup>(70)</sup> where only a calculated strength distribution can be compared with experiment.

The GDR is built on a collective  $1\hbar\omega$   $p$ - $h$  excitation. It is collective in the sense that it exhausts most of the  $E1$  sum rule strength. In the IBA model framework it can be described by coupling a  $P$ , a  $J^\pi = 1^-$ , boson to the system of  $s$ - and  $d$ -bosons. A general coupling Hamiltonian for this system can be written as

$$H = H_{sd} + \varepsilon_p \hat{n}_p + a_0 \hat{n}_d \hat{n}_p + a_1 L_d^{(1)} \cdot (P^\dagger \tilde{P})^{(1)} + a_2 Q_{sd} \cdot (P^\dagger \tilde{P})^{(2)} \quad (6.13)$$

where  $H_{sd}$  and  $Q_{sd}$  are the usual IBA Hamiltonian and quadrupole operator.

An interesting result is obtained in this model when the  $P$ -boson is coupled to an  $SU(3)$  boson core. In numerical calculations<sup>(87)</sup> it was observed that in this case the strength is distributed over only two states in the ratio 1:2, in the limit of a strong coupling. This result

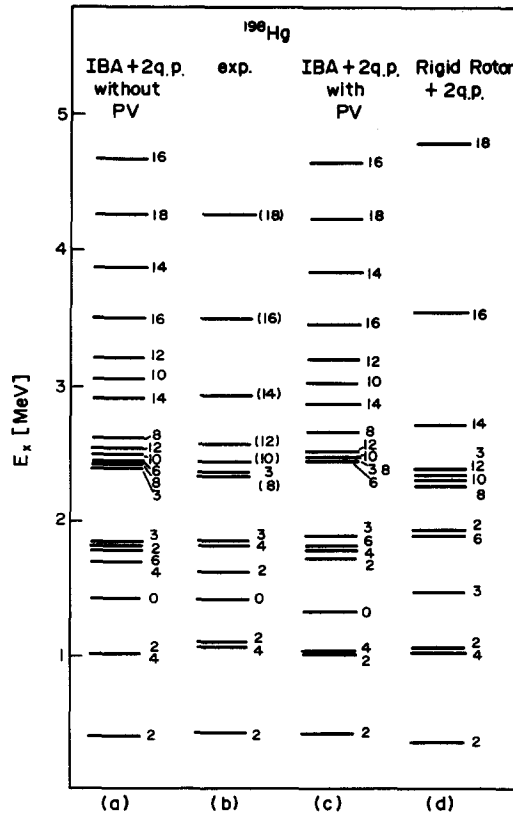


Fig. 22. Experimental<sup>(98)</sup> and calculated<sup>(91)</sup> spectrum of  $^{198}\text{Hg}$ .

is identical to what is expected in a geometrical model.<sup>(99)</sup> In Ref. 89 it is explained in terms of an approximate  $SU(3)$  symmetry in the combined system of  $s$ ,  $d$  and  $P$ -bosons. A detailed comparison<sup>(88)</sup> of the model predictions with data for  $^{168}\text{Er}$  shows an excellent agreement, not only for the total photon absorption cross section, but also for photon inelastic scattering.

One of the predictions of the model is that in the  $O(6)$  limit for the core Hamiltonian the strength is distributed over more than two collective states<sup>(87,89)</sup> while in the  $SU(5)$  limit one observes only a single slightly broadened peak<sup>(87)</sup> in the strength distribution. This implies that the spreading width of the GDR state will be considerably different for the three limits.

## 7. SUMMARY

The Hamiltonian of the IBFA model has been derived on the basis of a semi-microscopic theory, which is used to obtain a general structure of the boson-fermion interaction but where the strengths of the different components in the force are treated as freely adjustable parameters. In this way a model is obtained which has enough flexibility to describe a vast amount of experimental data using only a few (two or three) parameters. In the following only some of the major successes obtained and the major problems encountered in this model will be mentioned.

In several different microscopic approaches to the IBFA model an essentially similar structure for the boson–fermion interaction has been obtained. In phenomenological calculations where the strength of the different components in the force is adjusted a good agreement with experiment is obtained. The transition from a weak coupling particle–vibration spectrum to that of the strong coupling deformed Nilsson scheme is correctly reproduced.

Although microscopic calculations can account for the qualitative features of the IBFA model parameters obtained from phenomenological fits, their absolute magnitude is not yet understood. This situation is very much like that of the IBA model for even–even nuclei. In addition, the phenomenological calculations show some evidence that the structure of the operator for calculating single-particle transfer amplitudes is incomplete. Clearly the basic microscopic picture behind the IBFA model is qualitatively understood but several open problems still exist.

The boson–fermi symmetries are instrumental in understanding the structure in the complex spectra of odd-mass nuclei. They dictate simple analytic formulas for excitation energies and transition rates for nuclei which hitherto have been impossible to calculate in any model. The boson–fermi symmetries occur only when the boson–boson and boson–fermi interactions are in a specific relation to each other. The success of the symmetries in reproducing the spectra of odd-mass nuclei is an indication that these symmetries are much less broken than might have been expected *a priori* on the basis of the many restrictive conditions. This raises the interesting question, to be answered by a microscopic treatment, as to why the symmetry breaking is so small as experiment suggests. This apparently indicates that, in the nucleus, the collective and single-particle modes are closely related and should not be treated as two independent modes of excitation, as is usually done.

*Acknowledgements*—It is a pleasure to acknowledge many interesting discussions with A. Arima, R. Casten, J. Cizewski, D. H. Feng, R. Gilmore, F. Iachello, T. Otsuka, S. Pittel, I. Talmi, M. Vallieres, D. Warner and many others. Thanks are due especially to A. Dieperink for many stimulating discussions and a careful reading of the manuscript. The hospitality of the Kernfysisch Versneller Institute is gratefully acknowledged. This work was supported by the National Science Foundation under grant no. PHY-80-17605.

## REFERENCES

1. ARIMA, A. and IACHELLO, F., *Phys. Rev. Lett.* **35**, 1069 (1975).
2. ARIMA, A. and IACHELLO, F., *Ann. Phys.* **99**, 253 (1976).
3. ARIMA, A. and IACHELLO, F., *Ann. Phys.* **111**, 201 (1979).
4. ARIMA, A. and IACHELLO, F., *Ann. Phys.* **123**, 468 (1979).
5. JANSSEN, D., JOLOS, R. V. and DÖNNAU, F., *Nucl. Phys.* **A224**, 93 (1974).
6. See *Interacting Bosons in Nuclear Physics*, ed. F. IACHELLO, Plenum, New York (1979).
7. ELLIOTT, J. P. and WHITE, A. P., *Phys. Lett.* **97B**, 169 (1980).
8. MAINO, G., MARTINELLI, T., MENAPACE, E. and VENTURA, A., *Lett. Nuovo Cimento*, **32**, 235 (1981).
9. SCHOLTEN, O., IACHELLO, F. and ARIMA, A., *Ann. Phys.* **115**, 325 (1979).
10. CASTEN, R. F. and CIZEWSKI, J. A., *Nucl. Phys.* **A309**, 477 (1978).
11. STACHEL, J., VAN ISACKER, P. and HEYDE, K., *Phys. Rev.* **C25**, 650 (1982).
12. ARIMA, A., OTSUKA, T., IACHELLO, F. and TALMI, I., *Phys. Lett.* **66B**, 205 (1977).
13. OTSUKA, T., ARIMA, A., IACHELLO, F. and TALMI, I., *Phys. Lett.* **76B**, 139 (1978).
14. TALMI, I., *Nucl. Phys.* **A172**, 1 (1971).
15. OTSUKA, T., ARIMA, A. and IACHELLO, F., *Nucl. Phys.* **A309**, 1 (1978).
16. OTSUKA, T., Ph.D. Thesis, University of Tokyo, Japan (1979).
17. IACHELLO, F. and SCHOLTEN, O., *Phys. Rev. Lett.* **43**, 679 (1979).
18. ARIMA, A. and IACHELLO, F., *Phys. Rev.* **C14**, 761 (1976).
19. TALMI, I., *Comm. Nucl. Part. Phys.* **11**, 241 (1983).
20. RACAH, G., *Phys. Rev.* **63**, 367 (1943); **76**, 1352 (1949).

21. SCHOLTEN, O., *Phys. Rev.* **C28**, 1783 (1983).
22. LORAZO, B., *Phys. Lett.* **58B**, 257 (1975).
23. LORAZO, B., *Ann. Phys.* **92**, 95 (1975).
24. SCHOLTEN, O. and KRUSE, H., *Phys. Lett.* **125B**, 113 (1983).
25. KRUSE, H. and WILDENTHAL, B. H., *Bull. APS* **27**, 533 (1982); **27**, 725 (1982) and to be published.
26. SHIRLEY, V. S. and LEDERER, C. M., *Table of Isotopes*, LBL Press (1979).
27. SCHOLTEN, O. and PITTEL, S., *Phys. Lett.* **120B**, 9 (1983).
28. DE SHALIT, A. and TALMI, I., *Nucl. Shell Theory*, Academic Press, NY (1963).
29. PITTEL, S. and DUKELSKI, J., *Phys. Lett.* **128B**, 9 (1983).
30. OTSUKA, T., *Nucl. Phys.* **A368**, 244 (1981).
31. OTSUKA, T., *Proc. of the INS Symp. on Dynamics of Nuclear Collective Motion*, eds. K. OGAWA and K. TANABE, p. 382, Bando, Osaka, 1982.
32. SCHOLTEN, O., Ph.D. Thesis, University of Groningen, The Netherlands (1980).
33. DIEPERINK, A. E. L. and BIJKER, R., *Phys. Lett.* **116B**, 77 (1982).
34. TALMI, I., in: *Interacting Bose-Fermi Systems in Nuclei*, ed. F. IACHELLO, p. 329, Plenum Press, New York (1981).
35. GELBERG, A., *Z. Phys.* **A310**, 117 (1983).
36. DUVAL, P. D. and BARRETT, B. R., *Phys. Rev. Lett.* **46**, 1504 (1981); *Phys. Rev.* **C24**, 1272 (1981).
37. PITTEL, S., DUVAL, P. D. and BARRETT, B. R., *Ann. Phys.* **144**, 168 (1982).
38. BONSIGNORI, G., ALLAART, K. and VAN EGMOND, A., in: *Collective Bands in Nuclei*, ed. D. H. WILKINSON, Pergamon, Oxford (1982).
39. BORTIGNON, P. F., BROGLIA, R. A., BES, D. R. and LIOTTA, R., *Phys. Rep.* **30c**, 305 (1977).
40. VITTURI, A., in: *Interacting Bose-Fermi Systems in Nuclei*, ed. F. IACHELLO, p. 355, Plenum Press, New York (1981).
41. BROGLIA, R. A., MATSUYANAGI, K., SOFIA, H. M. and VITTURI, A., *Nucl. Phys.* **A348**, 237 (1980).
42. SCHOLTEN, O. and DIEPERINK, A. E. L., in: *Interacting Bose-Fermi Systems in Nuclei*, ed. F. IACHELLO, p. 343, Plenum Press, New York (1981).
43. BIJKER, R., private communication.
44. GINOCCHIO, J. N. and KIRSON, M. W., *Phys. Lett.* **44**, 1744 (1980). DIEPERINK, A. E. L. and SCHOLTEN, O., *Nucl. Phys.* **A346**, 125 (1980).
45. See BOHR, A. and MOTTELSON, B. R., *Nuclear Structure*, Vol. II, W. A. Benjamin, Reading, Massachusetts (1975).
46. KISSLINGER, L. S., *Nucl. Phys.* **78**, 341 (1966).
47. KURIYAMA, A., MARUMORI, T. and MATSUYANAGI, K., *Prog. Theor. Phys., Suppl.* **58**, 1 (1975).
48. DÖNAU, F. and HAGEMANN, U., *Nucl. Phys.* **A256**, 27 (1976).
49. DÖNAU, F. and FRAUENDORF, S., *J. Phys. Soc. Jpn.* **49**, suppl. p. 526 (1978).
50. SCHOLTEN, O., program package "ODDA", KVI internal report no. 255 (1980).
51. NILSSON, S. G., *Mat. Fys. Medd. Dan Vid Selsk* **29 no. 16** (1955).
52. HAMAMOTO, I., *Phys. Lett.* **106B**, 281 (1981). HAMAMOTO, I., *Phys. Lett.* **102B**, 225 (1981).
53. DÖNAU, F. and FRAUENDORF, S., in: *Nuclear Collective Dynamics*, eds. D. BUCERESCU, V. CEAUSESCU and N. V. ZAMFIR, p. 309, World Scientific (1982).
54. WOOD, J., private communication.
55. WILETS, L. and JEAN, M., *Phys. Rev.* **102**, 788 (1956).
56. IACHELLO, F., p. 273; SCHOLTEN, O., p. 285; VON BRENTANO, P., GELBERG, A. and KAUP, U., p. 303; CASTEN, R. F., p. 317, in: *Interacting Bose-Fermi Systems in Nuclei*, ed. F. IACHELLO, Plenum Press, New York (1981); WOOD, J., p. 451; and SCHOLTEN, O., p. 503, in: *Contemporary Research in Nuclear Physics*, eds. D. H. FENG et al., Plenum Press, New York (1981). CUNNINGHAM, M. A., *Phys. Lett.* **106B**, 11 (1981).
57. SCHOLTEN, O. and BLASI, N., *Nucl. Phys.* **A380**, 509 (1982).
58. *Nucl. Data Sheets* **25**, 113 (1978); **19**, 337 (1976); **19**, 33 (1976); **10**, 429 (1973); **15**, 409 (1975).
59. NAHAYAMA, H., CHIBA, J., SEKIMOTO, M. and NAKAI, K., *Nucl. Phys.* **A293**, 137 (1977).
60. DRACOLIS, G. D., LEIGH, J. R., SLOCOMBE, M. G. and NEWTON, J. O., *J. Phys.* **G1**, 853 (1975).
61. FLEISSNER, J. G., FUNK, E. G., VENEZIA, F. P. and MIHELICH, J. W., *Phys. Rev.* **C16**, 227 (1977).
62. LO BIANCO, G., MOLHO, N., MORONI, A., ANGIUS, S., BLASI, N. and FERRERO, A., *J. Phys.* **G5**, 697 (1979).
63. LO BIANCO, G., MOLHO, N., MORONI, A., BRACCO, A. and BLASI, N., *J. Phys.* **G5**, 219 (1979).
64. HESS, J., *Nucl. Phys.* **A142**, 273 (1970).
65. GÜNTHER, C. and SOARES, J. C., *Nucl. Phys.* **A257**, 1 (1976).
66. STRAUME, O., LØVHØIDEN, G. and BURKE, D. G., *Z. Phys.* **A290**, 67 (1979).
67. STRAUME, O., LØVHØIDEN, G. and BURKE, D. G., *Nucl. Phys.* **A266**, 390 (1976).
68. SCHOLTEN, O., *Phys. Lett.* **108B**, 155 (1982).
69. KRUSE, H., private communication.
70. SCHOLTEN, O., HARAKEH, M. N., VAN DER PLICHT, J., PUT, L. W., SIEMSEN, R. H., VAN DER WERF, S. Y. and SEKIGUCHI, M., *Nucl. Phys.* **A348**, 301 (1980).
71. BALANTEKIN, A. B., BARS, I., BIJKER, R. and IACHELLO, F., *Phys. Rev.* **C27**, 1761 (1983).
72. SUN, H. Z., FRANK, A. and VAN ISACKER, P., *Phys. Rev.* **C27**, 2430 (1983).



73. SUN, H. Z., FRANK, A. and VAN ISACKER, P., *Phys. Lett.* **124B**, 275 (1983).
74. SUN, H. Z., VALLIERES, M., FENG, D. H., GILMORE, R. and CASTEN, R. F., *Phys. Rev.* **C29**, 352 (1984).
75. WARNER, D. D., CASTEN, R. F., STELTZ, M. L., BORNER, H. G. and BARREAU, G., *Phys. Rev.* **C26**, 1921 (1982).
76. WARNER, D. D., *Phys. Rev. Lett.* **52**, 259 (1984); WARNER, D. D. and BRUCE, A. M., *Phys. Rev.* **C30**, 1066 (1984).
77. VERVIER, J. and JANSSENS, R. V. F., *Phys. Lett.* **108B**, 1 (1982).
78. BALANTEKIN, A. B., BARS, I. and IACHELLO, F., *Nucl. Phys.* **A370**, 284 (1981).
79. BALANTEKIN, A. B., Ph.D. Thesis, Yale University (1982).
80. IACHELLO, F., in: *Interacting Bose-Fermi Systems in Nuclei*, ed. F. IACHELLO, p. 365, Plenum Press, New York (1981).
81. LUKASIAK, J., KACZAROWSKI, R., JASTRZEBSKI, J., ANDRE, S. and TREHERNE, J., *Nucl. Phys.*, **A313**, 191 (1979).
82. SAKAI, M., *Quasi-Bands*, Inst. for Nuclear Study, Univ. of Tokyo (1982).
83. GOLDHOORN, P. B., HARAKEH, M. N., IWASAKI, Y., PUT, L. W., ZWARTS, F. and VAN ISACKER, P., *Phys. Lett.* **103B**, 291 (1981); VAN ISACKER, P., HEYDE, K., WAROQUIER, M. and WENES, G., *Phys. Lett.* **104B**, 5 (1981).
84. VAN ISACKER, P., *Interacting Bose-Fermi Systems in Nuclei*, ed. F. IACHELLO, p. 115, Plenum Press (1981).
85. HEYDE, K., VAN ISACKER, P., WAROQUIER, M., WENES, G. and SAMBATARO, M., *Phys. Rev.* **C25**, 3160 (1982).
86. VAN ISACKER, P., HEYDE, K., WAROQUIER, M. and WENES, G., *Nucl. Phys.* **A380**, 383 (1982).
87. MORRISON, I. and WEISSE, J., *J. Phys.* **G8**, 687 (1982).
88. SCHOLTZ, F. G. and HAHNE, F. J. W., *Phys. Lett.* **123B**, 147 (1983).
89. ROWE, D. J. and IACHELLO, F., *Phys. Lett.* **130B**, 231 (1983).
90. GELBERG, A. and ZEMEL, A., *Phys. Rev.* **C22**, 937 (1980); and GELBERG, A. and ZEMEL, A., in: *Interacting Bose-Fermi Systems in Nuclei*, ed. F. IACHELLO, p. 129, Plenum Press, New York (1981).
91. MORRISON, I., FAESSLER, A. and LIMA, C., *Nucl. Phys.* **A372**, 13 (1981).
92. YOSHIDA, N., ARIMA, A. and OTSUKA, T., *Phys. Lett.* **114B**, 86 (1982).
93. DUVAL, P. D. and BARRETT, B. R., *Phys. Lett.* **100B**, 223 (1981).
94. KONIJN, J., DE BOER, F. W. N., VAN POELGEEST, A., HESSELINK, W. H. A., DE VOIGT, M. J. A., VERHEUL, H. and SCHOLTEN, O., *Nucl. Phys.* **A352**, 191 (1981).
95. KROTH, R., BHATTACHERJEE, S. K., GÜNTHER, C., GUTTORMSEN, M., HARDT, K., HÜBEL, H. and KLEINRAHM, A., *Phys. Lett.* **97B**, 197 (1980).
96. YADAV, H. L., TOKI, H. and FAESSLER, A., *Phys. Rev. Lett.* **39**, 1128 (1977); *Phys. Lett.* **76B**, 144 (1978).
97. TOKI, H., NEERGÅRD, K., VOGEL, P. and FAESSLER, A., *Nucl. Phys.* **A279**, 1 (1977).
98. *Nucl. Data Sheets* **22**, 433 (1977).
99. DANOS, M., *Nucl. Phys.* **5**, 23 (1958); OKAMOTO, K., *Phys. Rev.* **110**, 143 (1958).
100. WARNER, D. D. and CASTEN, R. F., *Phys. Rev.* **C28**, 1798 (1983).
101. PIEPENBRING, R., SILVESTRE-BRAC, B. and SZYMANSKI, Z., *Nucl. Phys.* **A348**, 77 (1980).
102. MATSUYANAGI, K., *Prog. Theor. Phys.* **67**, 1441 (1982).